Article

Cell Host & Microbe

Intrahost Selection Pressures Drive Rapid Dengue Virus Microevolution in Acute Human Infections

Graphical Abstract

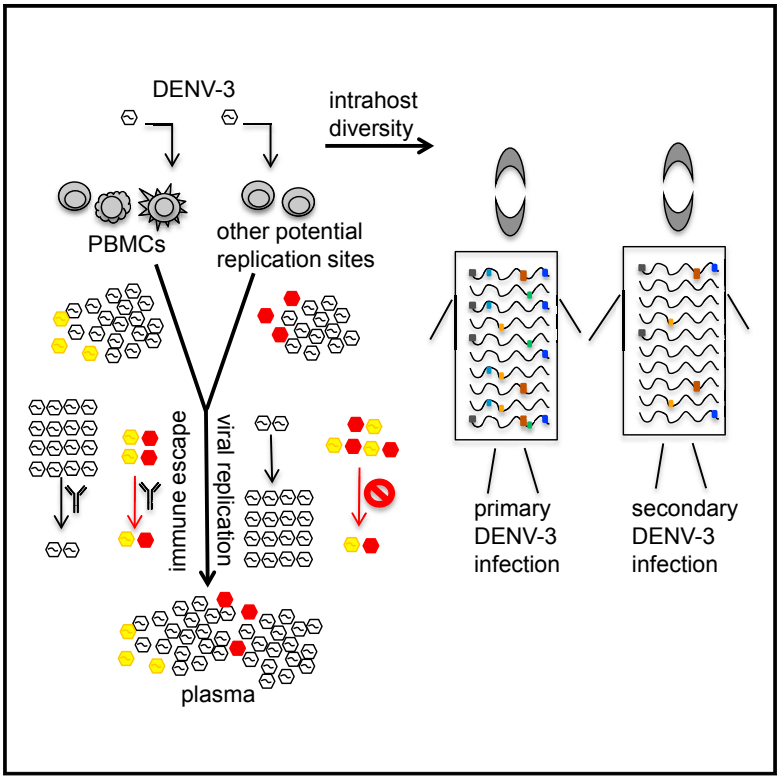

Authors

Poornima Parameswaran, Chunling Wang, Surbhi Bharat Trivedi, Meghana Eswarappa, Magelda Montoya, Angel Balmaseda, Eva Harris

Correspondence

eharris@berkeley.edu

In Brief

Dengue, caused by DENV-1 to -4, is a highly prevalent viral disease. Parameswaran et al. profile DENV-3 intrahost diversity in 77 patients, showing that intrahost virus microevolution occurs in PBMCs and potentially other replication sites. They find that intrahost variants, likely immune-escape hotspots, arise via convergent microevolution, yet are evolutionarily constrained by replication defects.

Highlights

- DENV-3 intrahost diversity was analyzed in PBMCs and/or plasma from 77 dengue patients
- Virus microevolution is shaped by immune pressure and replication sites including PBMCs
- Hotspots arose via convergent microevolution and are likely immune-escape variants
- Hotspot variants were evolutionarily constrained by replication defects

Parameswaran et al., 2017, Cell Host & Microbe 22, 400–410
September 13, 2017
http://dx.doi.org/10.1016/j.chom.2017.08.003

CellPress

Cell Host & Microbe
Article

Intrahost Selection Pressures Drive Rapid Dengue Virus Microevolution in Acute Human Infections

Poornima Parameswaran,[1,3] Chunling Wang,[1,3] Surbhi Bharat Trivedi,[1] Meghana Eswarappa,[1] Magelda Montoya,[1] Angel Balmaseda,[2] and Eva Harris[1,4,*]

[1]Division of Infectious Diseases and Vaccinology, School of Public Health, University of California, Berkeley, 185 Li Ka Shing Center, 1951 Oxford Street, Berkeley, CA 94720-3370, USA

[2]Laboratorio Nacional de Virología, Centro Nacional de Diagnóstico y Referencia, Ministry of Health, Managua 16064, Nicaragua

[3]These authors contributed equally

[4]Lead Contact

*Correspondence: eharris@berkeley.edu

http://dx.doi.org/10.1016/j.chom.2017.08.003

SUMMARY

Dengue, caused by four dengue virus serotypes (DENV-1 to DENV-4), is a highly prevalent mosquito-borne viral disease in humans. Yet, selection pressures driving DENV microevolution within human hosts (intrahost) remain unknown. We employed a whole-genome segmented amplification approach coupled with deep sequencing to profile DENV-3 intrahost diversity in peripheral blood mononuclear cell (PBMC) and plasma samples from 77 dengue patients. DENV-3 intrahost diversity appears to be driven by immune pressures as well as replicative success in PBMCs and potentially other replication sites. Hotspots for intrahost variation were detected in 59%–78% of patients in the viral Envelope and pre-Membrane/Membrane proteins, which together form the virion surface. Dominant variants at the hotspots arose via convergent microevolution, appear to be immune-escape variants, and were evolutionarily constrained at the macro level due to viral replication defects. Dengue is thus an example of an acute infection in which selection pressures within infected individuals drive rapid intrahost virus microevolution.

INTRODUCTION

Dengue virus (DENV) is a mosquito-borne *Flavivirus* with a single-stranded RNA genome that causes an estimated 390 million infections and up to 96 million dengue cases worldwide every year (Bhatt et al., 2013). There are four closely related serotypes of DENV (DENV-1 to DENV-4), each of which encodes three structural proteins (Capsid [C], pre-Membrane/Membrane [prM/M], and Envelope [E]) and seven non-structural (NS) proteins (NS1, NS2A, NS2B, NS3, NS4A, NS4B, NS5). Infections with DENV can result in a spectrum of clinical manifestations, ranging from asymptomatic infection to the debilitating acute febrile illness, dengue fever (DF), to the life-threatening dengue hemorrhagic fever/dengue shock syndrome (DHF/DSS) (WHO, 1997). Major determinants of dengue pathogenesis include virulence of the infecting DENV strain, host genetic factors, and pre-existing host immune responses from prior infection(s) with a different DENV serotype (Halstead and Yamarat, 1965; Messer et al., 2003; Nguyen et al., 2008; OhAinle et al., 2011; Rico-Hesse et al., 1997). In sequential infections, disease severity appears to be determined by a complex interplay of protective and enhancing components from pre-existing immunity to viral antigens (Halstead, 2009; Peiris and Porterfield, 1979; Rothman and Ennis, 1999). Such intricacies of the human immune response to DENV infection have made it difficult not only to identify the precise mechanisms that trigger progression to severe disease but also to engineer vaccines and therapeutics for combating the disease.

Replication of DENV within each host produces a population of genetically related but distinct genomes (referred to as intrahost diversity) due to the error-prone nature of the viral replicase, the RNA-dependent RNA polymerase (RdRP) (Domingo and Holland, 1997). These intrahost variants are thought to serve as templates on which evolutionary mechanisms act to shape variation at the consensus level between hosts (i.e., interhost diversity), leading to the emergence of genetically distinct strains and genotypes of DENV. Genetic variations in intrahost populations have been proposed to influence disease outcome and pathogenesis in chronic human infections with RNA viruses such as HIV and hepatitis C virus (HCV) (Farci et al., 2002; Joos et al., 2005; Lee et al., 2008; Moreau et al., 2008; Sullivan et al., 2007), which provide considerable time frames (months to years) for discernible virus evolution in response to intrahost selection pressures. Similar observations have also been reported in chronic infections with influenza virus and norovirus, viruses that are usually associated with acute infections (Bull et al., 2012; Debbink et al., 2014; Rogers et al., 2015; Valkenburg et al., 2013). These studies have characterized the emergence of individual variants associated with immune evasion or drug resistance. Unlike chronic infections, only a handful of studies have reported on the evolutionary mechanisms and viral genetics driving virus evolution in acute human infections such as Ebola (Gire et al., 2014; Ni et al., 2016), chikungunya (Stapleford et al., 2016), influenza A (Sobel Leonard et al., 2016), Middle East

Table 1. Summary of Samples Used in This Study

Sample Type[a]	Year of Collection	Disease Severity	Immune Status	No. of Samples[b]	No. of Paired Samples[b]
PBMCs	2009–2010	DF	primary	32	11
			secondary	23	9
		DHF/DSS	primary	5	0
			secondary	8	2
Plasma	2009–2010	DF	primary	16	11
			secondary	13	9
		DHF/DSS	primary	0	0
			secondary	2	2

[a]PBMC and plasma samples (including 53 primary and 46 secondary samples) were obtained from individuals aged 6 months to 14 years who were enrolled in the hospital-based pediatric dengue study and tested positive for DENV-3.

[b]Only nucleotide loci with coverage of ≥1,000 reads and locus-specific Sanger quality scores of ≥30 were considered for calculating genome coverage. Samples with ≥50% genome coverage are reported.

respiratory syndrome (Park et al., 2016), and dengue (Paramesworan et al., 2012; Rodriguez-Roche et al., 2016; Sessions et al., 2015; Sim et al., 2015; Thai et al., 2012), where virus evolution is severely constrained by time (days to weeks). Consequently, limited information exists about the fitness and pathogenesis profiles of individual intrahost DENV variants that emerge in acute human infections. Information on intrahost viral diversity can provide new perspectives in assessing infection outcome, disease pathogenesis, and vaccine or therapeutic efficacy in individuals with dengue or other closely related viral infections such as Zika.

In this study, we employ a whole-genome segmented amplification approach coupled with high-throughput sequencing to profile intrahost viral diversity across the entire coding region of the DENV-3 genome with considerable depth of coverage. Using snapshots of DENV-3 intrahost diversity in 31 plasma and 68 peripheral blood mononuclear cell (PBMC) samples from 77 individuals (including 22 with paired plasma and PBMC samples) enrolled in a prospective pediatric hospital-based study in Nicaragua, we demonstrate that DENV-3 diversification in human acute dengue (microevolution) is shaped by convergent selection pressures, including pre-existing immunity, and possibly by replication in sites other than PBMCs, while it is constrained by severe defects in replicative ability.

RESULTS AND DISCUSSION

Samples and Methods

All PBMC and plasma samples used in this study were collected on the first day of presentation from individuals aged 6 months to 14 years with primary (1°; 53 samples) or secondary (2°; 46 samples) acute, symptomatic DENV-3 infection during the 2009–2010 epidemic season in Managua, Nicaragua (Tables 1 and S1) (Narvaez et al., 2011). The majority of PBMC (82%) and plasma (91%) samples were from individuals who presented with DF. The rest of the PBMC (18%) and plasma (9%) samples were from individuals who presented with DHF/DSS. Supporting clinical information is provided in Table S1.

The DENV-3 genome was amplified via reverse transcription and PCR using sequence-specific primer pairs to generate 12 overlapping amplicons per sample (Figure S1A). Multiplexed libraries for high-throughput sequencing were constructed from pooled amplicon mixes and sequenced on an Illumina HiSeq 2000 platform to yield 150-nucleotide (nt) paired-end reads in forward (read 1) and reverse (read 2) orientations. Reference genomes were reconstructed for each sample using *Bowtie2* (Langmead and Salzberg, 2012) and *SAMtools* (Li et al., 2009), and in-house python scripts were used to calculate variation at the nucleotide, codon, and amino acid levels for each locus in the DENV-3 coding region (see STAR Methods). After filtering for coverage (≥1,000 reads) and Sanger quality scores (≥30), median coverage per codon locus was 22,975 and 20,024 for read 1 and read 2 datasets, respectively. Only samples with ≥50% coverage of the DENV-3 genome were retained for downstream analyses; 68 PBMC and 31 plasma samples from 77 individuals, including paired PBMC-plasma datasets from 22 individuals, passed the threshold for genome coverage. Coding-region coverage in these samples varied between 50.7% and 99.9% (median of 98.9%) for both read 1 and read 2 datasets combined (Table S1).

Percent variant diversity at nucleotide, codon, and amino acid loci was calculated as the percent of reads spanning each coordinate that was different from consensus. Nucleotide- and codon-level diversities provide aggregate measures of both non-synonymous and synonymous mutations (i.e., mutations that do and do not change amino acid encoding, respectively), while amino acid diversity only captures non-synonymous mutations. In our study, variant abundances of ≥1.0% were reproducible across replicates (see STAR Methods) and were considered variants of high confidence. Unless otherwise specified, we used high-confidence variants for investigating diversity patterns. Samples from both sexes were included in all intrahost diversity comparisons; no significant differences between sexes were observed for any of the calculated DENV-3 intrahost diversity metrics (data not shown).

Intrahost Immune Pressures Shape DENV-3 Diversity in Acute Human Infections

We evaluated snapshots of intrahost diversity in samples from distinct subsets of individuals with 1° (53 samples) or 2° (46 samples) dengue to assess the effects of immune-driven selection pressures on intrahost DENV evolution. We compared the percent loci per protein that are variant in any sample between 1° and 2° dengue and found significantly fewer unique variant loci in 2° dengue cases, both in PBMC (Figure 1A; left panel, $p < 0.001$) and plasma (Figure 1A; right panel, $p < 0.01$) samples. These observations were not due to systematic disparities in the yields of viral RNA, since measures of genome equivalents (GE) per milliliter of extracted viral RNA were not significantly different between 1° and 2° cases for both PBMC and plasma samples (Figure 1B; left and right panels). Thus, DENV-3 appears to be evolving at fewer distinct loci genome-wide in 2° dengue compared with 1° dengue, suggesting that virus evolution is constrained by pre-existing immune pressures in 2° dengue. In addition, we examined the locations of unique variant loci on the exposed and membrane-associated surfaces of the E protein, which is a prominent target for antibody-mediated immunity in

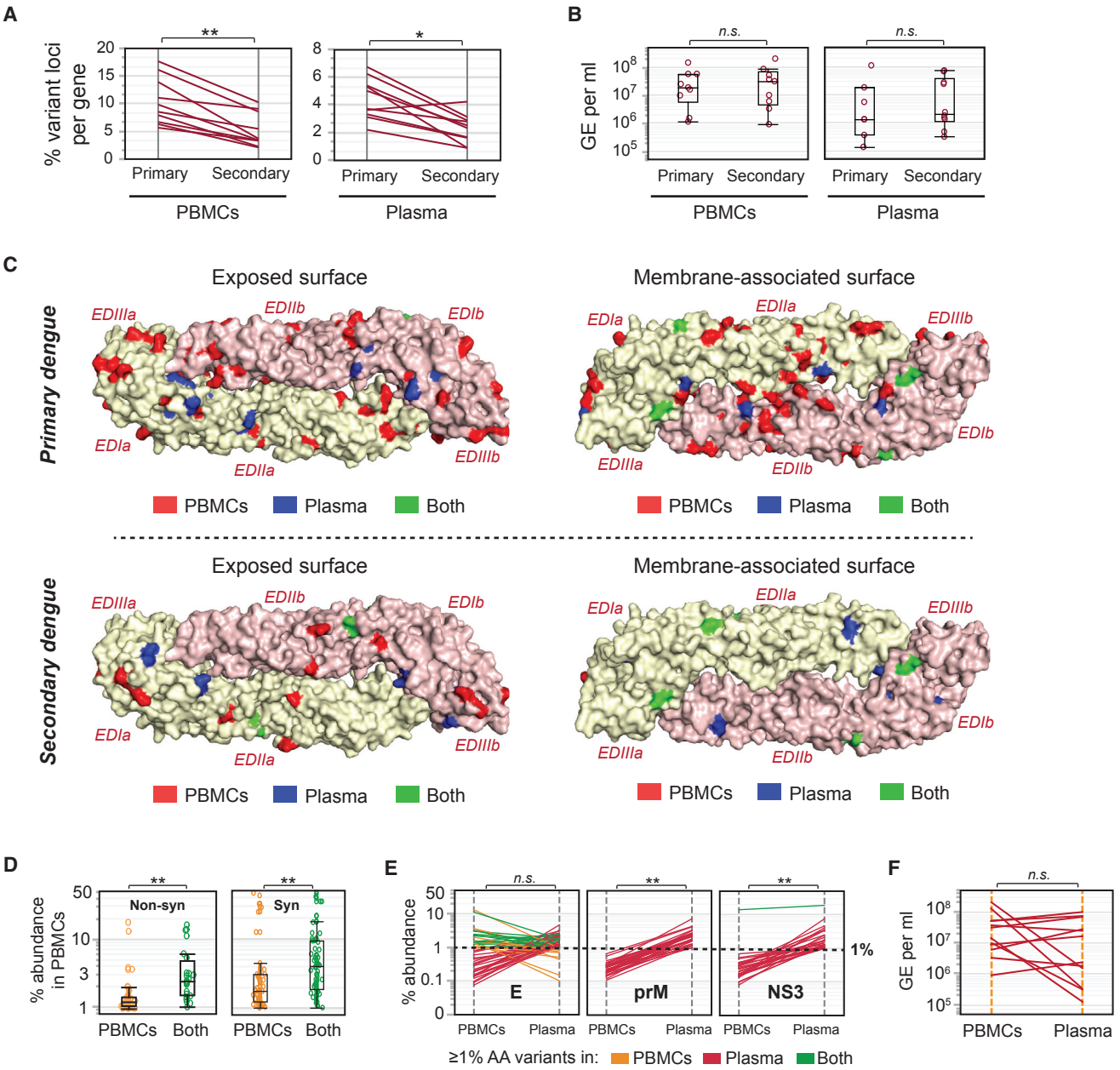

Figure 1. DENV-3 Intrahost Diversity Is Shaped by Selection Pressures

(A) Percent unique loci per protein with amino acid diversity, calculated as the percent of amino acids in a protein that show ≥1% variation, in PBMC (left panel) and plasma (right panel) samples from 53 individuals with 1° and 46 individuals with 2° dengue. *p ≤ 0.01, **p ≤ 0.001 (Wilcoxon signed-rank test). Each line represents one protein.

(B) Comparisons of genome equivalents per milliliter (GE/mL) of extracted RNA in 53 1° and 46 2° cases from PBMC (left panel) and plasma (right panel) samples, median ± SD, boxes represent 25th and 75th percentiles and whiskers are 10th and 90th percentiles. n.s., non-significant (Wilcoxon test for unpaired samples).

(C) All loci with ≥1% variation at the amino acid level, superimposed on the exposed surface (left panel) or the membrane-associated surface (right panel) of the DENV-3 E protein homodimer (PDB: 1UZG). Amino acids are colored according to whether they exhibit diversity in PBMC samples only (PBMCs, red), in plasma samples only (Plasma, blue), or in both PBMCs and plasma (Both, green). Data are shown separately for 53 1° (top panel) and 46 2° (bottom panel) dengue cases. *EDIa*/*b*, *EDIIa*/*b*, *EDIIIa*/*b* represent E domains I, II, and III from monomer chains a and b, respectively.

(D) Percent amino acid variants for loci that exhibit diversity in PBMCs only (PBMCs), compared with loci that exhibit diversity in both PBMCs and plasma (Both), median ± SD, boxes represent 25th and 75th percentiles and whiskers are 10th and 90th percentiles. In the left panel, the y axis represents the percent abundance of non-synonymous variants in PBMCs. In the right panel, the y axis represents the percent abundance of synonymous variants in PBMCs. **p ≤ 0.0001 (Wilcoxon test), n = 22 paired PBMC and plasma samples.

(E) Protein-specific comparisons of percent amino acid variants in 22 paired PBMC and plasma samples, colored by whether individual loci display ≥1% amino acid diversity in PBMC samples only (yellow), in plasma samples only (red), or in both PBMC and plasma samples (green). Data are shown for the two proteins

(legend continued on next page)

human dengue. We detected fewer unique variant loci across all samples in 2° dengue cases compared with 1° cases (Figure 1C; top and bottom panels) on both the exposed and the membrane-associated surfaces of E; much of this difference was contributed by PBMC-specific variant loci. Thus, consistent with genome-wide differences between 1° and 2° dengue, the breadth of the viral variant repertoire in E appears to be reduced in 2° dengue compared with 1° dengue. Such global differences in viral composition between naive individuals and individuals with pre-existing immunity to DENV indicate that the extent of diversity in the intrahost DENV-3 population is directed by the immune repertoire during acute dengue in humans. Further studies investigating particular epitopes will help resolve the specificities of pre-existing immune pressures contributing to differential rates of viral microevolution in 1° and 2° dengue.

Selection Pressures Shape DENV-3 Microevolution in Plasma

We used patterns of DENV-3 intrahost diversity in paired PBMC and plasma samples from a subset of 22 individuals to assess the role of selection pressures mediated by human immune pathways or virion intracellular replicative success in shaping differences in DENV variants at the PBMC-plasma (i.e., intracellular-extracellular) interface and to explore the relative contributions from PBMCs and other potential viral replication sites to circulating virion populations in plasma.

We examined the percent abundance of non-synonymous variants in PBMCs and plasma, binning loci by whether variants were found at levels $\geq$1% in PBMCs only (PBMCs), or in both PBMC and plasma samples (Both). The median percent abundance of variant DENV-3 genomes that were found in PBMCs only was significantly lower than the median percent abundance of variant genomes found in both PBMCs and plasma, for both non-synonymous and synonymous variants (Figure 1D, left and right panels, $p < 0.0001$). Thus, variants that appear in both PBMCs and plasma are more abundant than variants that are restricted to PBMCs, suggesting that DENV variants found in plasma have been selected based on their intracellular replicative success in PBMCs.

We also found evidence for immune-driven selection pressures shaping differences between plasma and PBMC DENV populations. In particular, significantly higher abundances for non-synonymous variants were observed in plasma compared with PBMCs for the prM/M and NS3 proteins (Figure 1E, $p < 0.0001$), which are major targets of the human B cell and T cell immune responses, respectively (de Alwis et al., 2014; Dejnirattisai et al., 2010; Rivino et al., 2013; Simmons et al., 2005; Weiskopf et al., 2013).

Furthermore, we observed many dissimilarities between PBMCs and plasma DENV populations that could not be attributed to replication defects or immune pressure mechanisms. For instance, minimal intersection was detected in the locations of variant loci on the highly antigenic E protein (Figure 1C, green loci), as well as in other proteins (Figures 1E and S2A), inferred from the presence of fewer green lines representing loci with $\geq$1% amino acid variants in both PBMC and plasma samples, compared with orange and red lines representing loci with $\geq$1% amino acid variants in PBMC or plasma samples, respectively. These findings were not due to differences in the depth of sequencing coverage (data not shown), or in the number of viral copies used as input for generating sequencing libraries (Figure S2B), because these parameters were comparable between paired PBMC and plasma samples. These observations of large-scale differences between plasma and PBMC DENV variant populations, when taken together with prior knowledge from human autopsy studies about the existence of significant non-PBMC compartments for viral replication in phagocytes, lymph node, spleen, alveolar macrophages in lung, and perivascular cells in brain (Aye et al., 2014; Balsitis et al., 2009; Jessie et al., 2004), suggest contribution to plasma DENV populations from replication compartments other than PBMCs.

Hotspots for DENV-3 Intrahost Diversity in Acute Human Dengue

We next sought to identify hotspots for intrahost viral diversity, defined as loci with detectable intrahost diversity in multiple hosts, in PBMC and plasma samples from individuals with DENV-3 infection. Hotspots may arise *de novo* within each host due to convergent selection pressures, or may be attributed to the co-transmission of wild-type (WT) and variant viruses within a host population. The probability of detecting diversity hotspots due to selection pressures has been assumed to be low in acute human dengue (Descloux et al., 2009; Lin et al., 2004; Parameswaran et al., 2012; Thai et al., 2012; Wang et al., 2002a, 2002b), primarily because of the time constraint (8–14 days) on virus evolution within hosts.

We analyzed percent variant abundance together with percent prevalence of variants at each codon locus (depicted by the color and size of each data point) across the entire DENV-3 coding region and found that very few codon loci were hotspots for intrahost diversity in PBMC and plasma samples (Figure 2A, top and bottom panels, respectively). However, prominent hotspots for diversity were identified in the majority (59%–78%) of samples at three codon coordinates: (1, 2) 214 and 215, corresponding to amino acids 100 and 101 in the membrane portion of prM/M (hereafter prM_{100} and prM_{101}), and (3) 595, corresponding to amino acid 315 in the highly conserved AB-loop region in E Domain III (E_{315}) (Figures 2A and 2B). To confirm the presence of the more abundant E_{315} variant, we designed primers that specifically targeted and amplified either WT or E_{315} DENV RNA and validated the specificity of these primers using RNA from WT or E_{315} variant viruses (Figure S3A). We tested a subset of seven serum samples used in this study and were able to directly detect the E_{315} hotspot variant at various levels in all seven clinical samples (Figure S3B).

The dominant variants at these hotspots were identical across samples (Figure S2C) and exhibited altered amino acid sequence compared with consensus: (1) glycine to serine at

(prM/M and NS3) that exhibit significant differences in % amino acid (AA) variants between PBMCs and plasma. All other proteins (including E, which is shown as an example) exhibit no significant differences in % AA variants between PBMCs and plasma. **$p \leq 0.0001$, n.s., non-significant (Wilcoxon signed-rank test). (F) Comparisons of genome equivalents per milliliter (GE/mL) of extracted RNA in 12 paired PBMC and plasma samples. n.s., non-significant (Wilcoxon signed-rank test for paired samples).

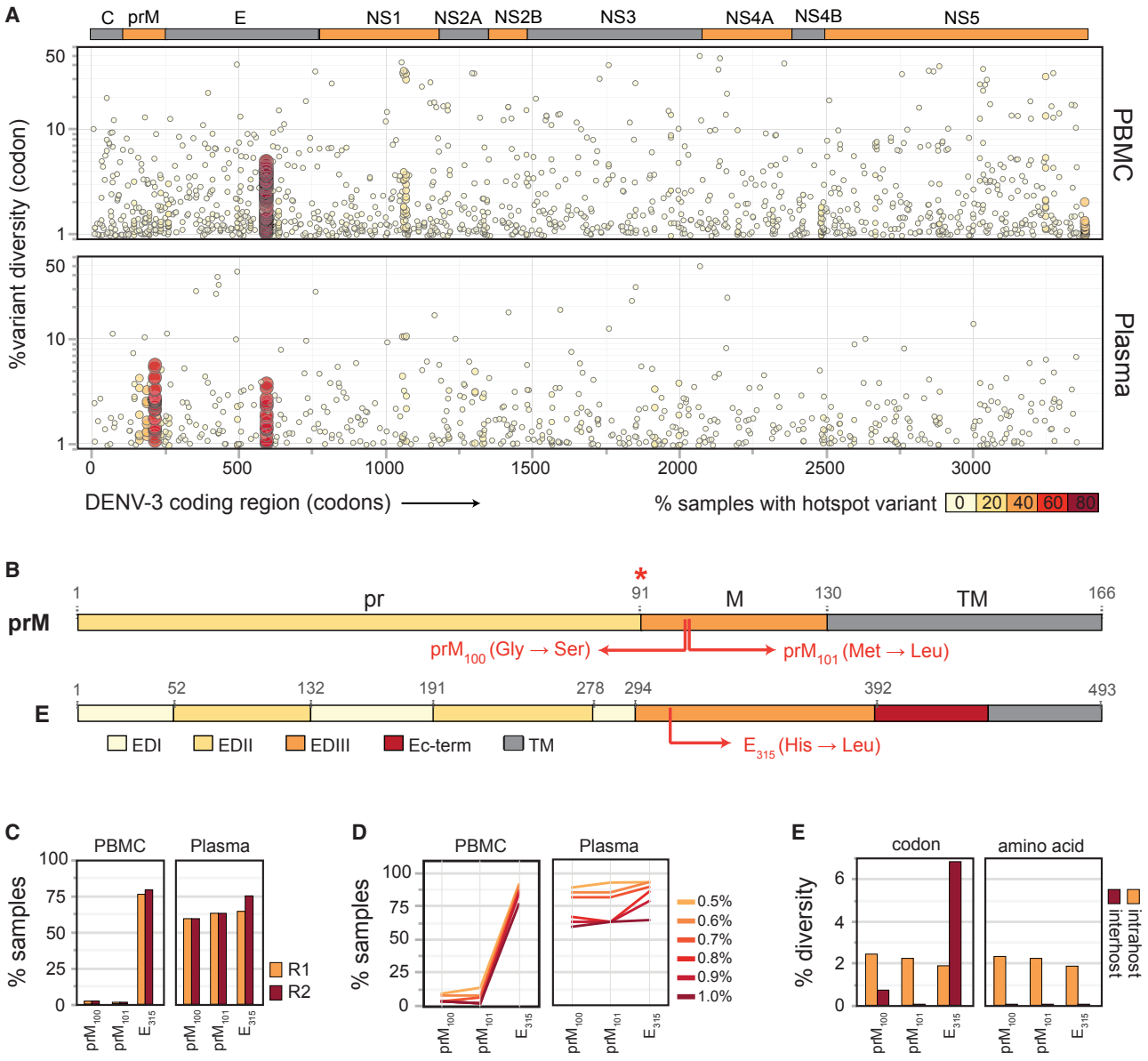

Figure 2. Hotspots for Intrahost Diversity in the DENV-3 Genome

(A) Percent intrahost codon diversity (y axis) across the coding region of DENV-3 (x axis) in 68 PBMC (top panel) and 31 plasma (bottom panel) samples; each data point is colored according to the number of samples in which ≥1% intrahost diversity is detected at that locus.

(B) Major variants at the hotspot loci in prM/M (top) and E (bottom). Red asterisk, furin cleavage site.

(C) Prevalence of major hotspot loci (i.e., loci with ≥1% variant abundance in ≥50% of samples) in 68 plasma (right panel) and 31 PBMC (left panel) samples in both read orientations (read 1 in yellow and read 2 in red).

(D) Percent samples with diversity at each hotspot locus, shown for increasing cutoffs for percent intrahost codon diversity, in the 68 PBMC (left panel) and 31 plasma (right panel) datasets.

(E) Average percent intrahost (yellow) and percent interhost (red) diversity in codon (left panel) or amino acid (right panel) coordinates for each hotspot locus. Interhost diversity was calculated across all global DENV-3 isolates for which full-genome sequences were available (n = 690).

prM_{100}, (2) methionine to leucine at prM_{101}, and (3) histidine to leucine at E_{315} (Figure 2B). prM_{100} and prM_{101} variants were significantly more prevalent in plasma (59.3% and 62.9%, respectively), compared with PBMC samples (2.9% and 1.4%, respectively) ($p < 0.0001$, Fisher's exact test), while the E_{315} variant was highly prevalent in both PBMC (77.6%) and plasma (69.7%) samples (Figure 2C, average of read 1 and read 2 values). Hotspots detected were not PCR artifacts from the amplicon and library preparation (data not shown). Even at lower thresholds of ≥0.5% variant abundance, the prM_{100} and prM_{101} variants were only detected in a small number of PBMC samples (8.8%–13.2% of samples; Figure 2D). The E_{315} variants thus appear to originate in PBMCs (in addition to other cell types), whereas it is conceivable that the prM_{100} and prM_{101} variants

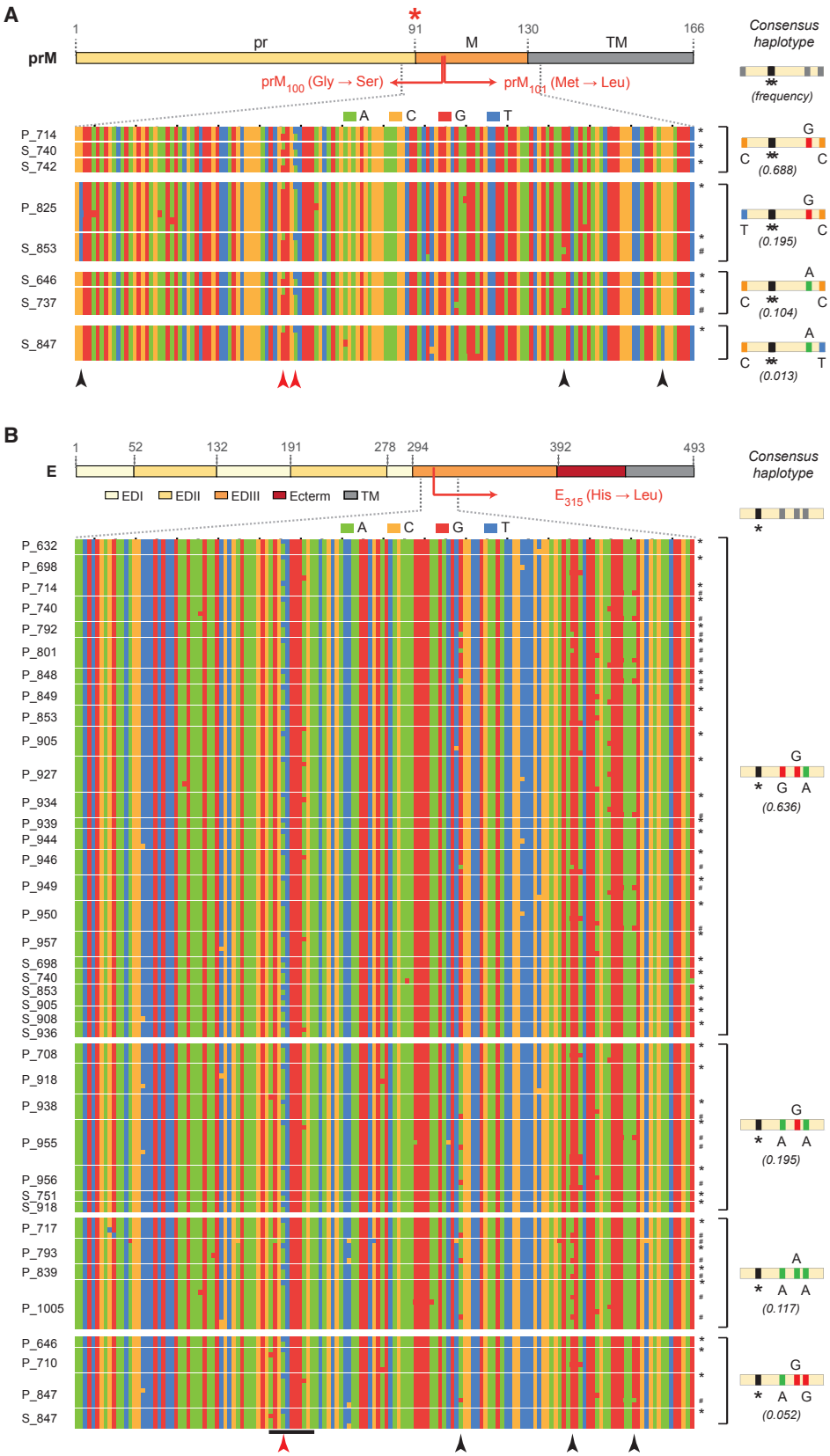

(legend on next page)

arise in viral replication sites distinct from PBMCs, although we have not ruled out the possibility that these variants arose in PBMCs and are simply enriched in the extracellular environment. The $prM_{100,101}$ and E_{315} variants constitute 2.2% and 1.9%, respectively, of an estimated 1.2×10^7 GE/mL of circulating viral populations in plasma (extrapolated from Figure 1F; median yield of 1.2×10^6 GE in 50 μL of RNA extracted from 100 μL of plasma) from individuals with detectable levels (≥1.0%) of these variants (Figure S2C, median abundances). We also analyzed interhost diversity in 690 full-length DENV-3 consensus genomes (GenBank) and found that even though DENV-3 exhibited codon-level diversity at prM_{100} and E_{315} (Figure 2E, left panel, red bars), virus populations were invariant in the interhost amino acid sequence at all three hotspots (Figure 2E, right panel, red bars, and Table S2), suggestive of macro-evolutionary (i.e., consensus-level) constraints at these loci. In addition to major hotspots, we detected several minor hotspots, defined as loci with 1.0% or higher variant abundance in ≥10% of samples, in both PBMC and plasma samples (Figure S2D, all minor hotspots marked with ^). Of these minor hotspots, only one (codon 1071 in polyprotein) appeared to be shared between PBMC and plasma samples at a diversity threshold of 1.0% (Figure S2D). All minor hotspots (loci marked with ^) exhibited interhost diversity at the codon level (Figure S2E, left panel, red line, and Table S2), but interhost amino acid diversity was only observed at five out of nine minor hotspots (Figure S2E, right panel, red line, and Table S2). Overall, our findings demonstrate that hotspots for intrahost viral diversity can be detected in acute human dengue. Furthermore, the presence of hotspot variants at macroevolutionarily conserved loci highlight the importance of host-specific selection pressures in DENV-3 intrahost evolution.

Convergent Evolution at Major Hotspot Loci

We next explored linkage patterns between polymorphisms in the sequences of reconstructed haplotypes spanning the $prM_{100,101}$ and E_{315} major hotspot loci to identify whether (1) variants at the prM_{100} and prM_{101} hotspot loci were present on the same viral genome, and (2) viruses with variation at the $prM_{100,101}$ and E_{315} hotspots arose *de novo* in different samples due to convergent selection pressures, or were present in multiple hosts due to co-transmission with consensus viral genomes. In samples with detectable levels of both prM variants at the population level, we observed that all haplotypes with the prM_{100} variant also included the prM_{101} variant (and vice versa), demonstrating that the prM variants were linked, i.e., present on the same variant viral genome (Figure 3A, red arrowheads). Moreover, we identified haplotypes with variants at only one prM hotspot (Figure S2F), which implied that DENV-3 was evolving independently at each of the prM_{100} and prM_{101} hotspots. The $prM_{100,101}$ variant thus appears to be the result of sequential evolution at prM_{100} and prM_{101} on the same viral genome. Our haplotype analysis also revealed significant interhost diversity at three loci proximal to the $prM_{100,101}$ and E_{315} hotspots (Figures 3A and 3B; black arrowheads). Four different haplotypes with a wide range of frequencies were detected among the consensus genomes in our samples, each with unique combinations of nucleotide diversity at these loci (Figures 3A and 3B, and Table S3). Nucleotides at all three polymorphic loci were 100% concordant between the dominant WT consensus genome and the prM/M or E variant genome for all samples (Figures 3A and 3B and Table S3; variant genomes marked with *). This was true even for samples with low-frequency consensus haplotypes (C-A-T and A-G-G haplotypes for prM/M and E, respectively), and for samples in which mixed infections with multiple WT haplotypes were detected (Figures 3A and 3B; genomes marked with #). The genetic concordance between WT and variant haplotypes in our samples strongly support the independent emergence and/or expansion of these hotspot variants within each individual, although we cannot completely exclude contributions from co-circulating variants at the $prM_{100,101}$ and E_{315} loci. Taken together, our observations indicate that variants at the $prM_{100,101}$ and E_{315} hotspot loci arose by convergent evolution during acute dengue, in at least four independent events, corresponding to the presence of the variants in four distinct haplotypes.

Replication Phenotypes and Origins of Hotspot Variants

The four-plasmid reverse genetics approach (Messer et al., 2012) was used to engineer chimeric infectious clones containing non-structural genes from a 1989 Sri Lankan DENV-3 isolate (GenBank: JQ411814.1) and either (1) Nicaraguan consensus sequence for the structural genes (WT), (2) WT Nicaraguan consensus with the Gly100Ser and Met101Leu mutations in the membrane portion of prM/M ($prM_{100,101}$ mutant), or (3) WT Nicaraguan consensus with the His315Leu mutation in the AB loop in E (E_{315} mutant). We evaluated the replication phenotypes of WT and mutant viruses in C6/36 mosquito cells by directly competing each mutant virus with WT virus in co-infection experiments (Quiner et al., 2014). Viral RNA mixtures from the input and from cellular supernatants collected 3, 4, and 5 days post infection (d.p.i.) were sequenced by the Sanger method to capture ratios of WT and mutant nucleotides at the $prM_{100,101}$ and E_{315} hotspots using the polySNP program. The replicative index, calculated as the $\log_2$ value of relative levels of WT and mutant viruses in the supernatant compared with relative levels in the input, was negative for $prM_{100,101}$ or E_{315} mutant viruses at 3–5 d.p.i., indicating that both mutants were replication defective in C6/36 cells compared with WT (Figure 4A). In addition, we assessed the replication phenotypes of WT and mutant viruses in a human monocytic U937 cell line that expresses DC-SIGN, a co-receptor for DENV entry (Tassaneetrithep et al., 2003) (U937-DC-SIGN). Single infections were performed in

Figure 3. Sequence Diversity in Reconstructed Haplotypes Spanning the Intrahost Diversity Hotspots in prM/M and E

Color-coded nucleotide diversity in regions flanking intrahost diversity hotspots in (A) prM/M and (B) E; each row represents a unique reconstructed haplotype with the hotspot variant in 8 PBMC/plasma samples for the *prM/M* hotspot and 39 PBMC/plasma samples for the *E* hotspot (samples delineated by thin white lines). Consensus haplotypes and their observed frequencies across all Nicaraguan samples are shown on the left, separated by thick white lines. Haplotypes with the $prM_{100,101}$ and E_{315} variants are denoted with asterisks (*), WT variant haplotypes distinct from the consensus haplotype are marked with #, and underlined loci in B represent the AB-loop region containing the E hotspot. Red asterisk, furin cleavage site. Red arrowheads, prM and E hotspot variants. Black arrowheads, other variants present at >1% abundance.

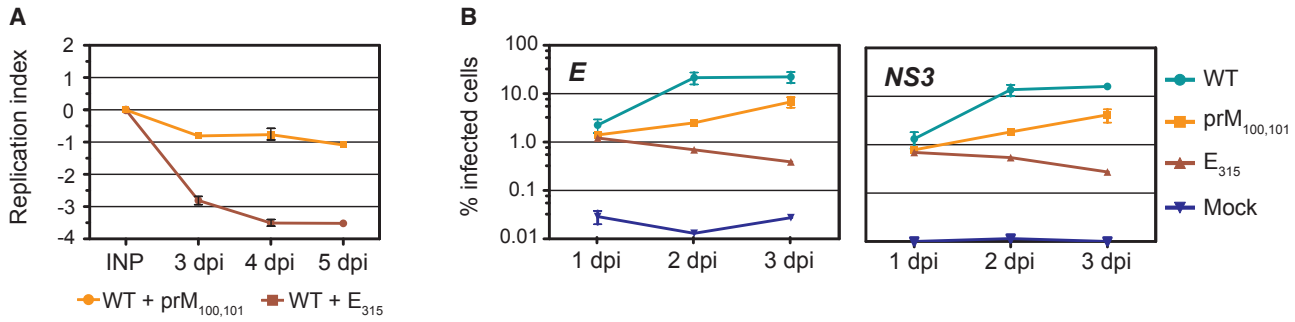

Figure 4. Phenotypic Differences between Wild-Type, $prM_{100,101}$, and E_{315} Viruses

(A) C6/36 cells were infected with a mixture containing WT virus and the $prM_{100,101}$ (yellow) or E_{315} (red) mutant viruses. The replication index was measured as the log_2 value of relative levels of mutant and WT genomes in the supernatant at 3–5 d.p.i., compared with the corresponding ratios in the input. A negative index indicates that the replicative ability of mutant virus is lower than WT virus.

(B) U937-DC-SIGN cells were mock-infected (mock, blue) or infected with WT (aqua), $prM_{100,101}$ (yellow), and E_{315} (red) viruses, fixed, and stained with anti-E (left panel) and anti-NS3 (right panel) antibodies at various time points post infection. All data points for (A and B) represent the average of two independent experiments, mean ± SD.

U937-DC-SIGN cells with 625 GE/cell each of WT, $prM_{100,101}$, and E_{315} viruses. All three viruses were able to establish infection in U937-DC-SIGN cells; however, the percent of infected cells was considerably reduced in infections with $prM_{100,101}$ and E_{315} variants compared with WT virus at 1, 2, and 3 d.p.i., as determined with both anti-E and anti-NS3 antibodies (Figure 4B, left and right panels, respectively). No revertants were detected at 3 d.p.i. with either variant (data not shown). The E_{315} variant also exhibited a temperature-sensitive (32°C versus 37°C) plaquing phenotype on baby hamster kidney (BHK-21) cells with better plaquing at 32°C, whereas the $prM_{100,101}$ variant plaqued relatively well at 37°C (Figure S4). Our results thus demonstrate that the $prM_{100,101}$ and E_{315} mutant viruses establish infections in C6/36 mosquito cells, U937-DC-SIGN human cells, and in BHK-21 mammalian cells with considerably reduced efficiencies due to the deleterious effects of these mutations on viral replicative ability.

The $prM_{100,101}$ and E_{315} mutant viruses do not exhibit any defects in entry and behave similar to WT virus, as demonstrated by directly comparing entry capabilities of the three viruses using U937-DC-SIGN cells at 37°C (Figure S5), suggesting that the replication defect for both $prM_{100,101}$ and E_{315} mutant viruses is downstream of virus entry. We do not anticipate that these mutations have a direct impact on viral RNA replication, as none of the DENV structural proteins, except RNA elements in the Capsid gene (Byk and Gamarnik, 2016; Clyde et al., 2008; de Borba et al., 2015; Friebe et al., 2011; Selisko et al., 2014), have been implicated in a direct role in RNA replication. In studies by Zheng et al. (2014), mutations at prM_{98} in DENV-1 were shown to result in impaired prM processing and decreased viral infectivity. prM_{100} and prM_{101} are situated only 2–3 amino acids away from prM_{98}, and given the absence of entry and replication defects, we hypothesize that the $prM_{100,101}$ hotspot mutations likely impair prM processing and DENV infectivity, by a mechanism similar to prM_{98} (Zheng et al., 2014). Even though prM antibodies have been identified by several groups (Beltramello et al., 2010; Dejnirattisai et al., 2010), the immune pressures driving evolution at the prM/M locus are poorly understood, and the origin of the $prM_{100,101}$ variant viruses remains elusive. In contrast, significantly more is known about the functionalities and antigenicity of loci in the E protein, and specifically the E_{315} locus. Previous studies have shown that E_{315} plays a pH-sensing role in mediating viral fusion with the endosome at the post-entry stage (Nelson et al., 2009), suggesting that viruses with the E_{315} hotspot mutation are likely impaired at the stage of viral membrane fusion with the endosomal membrane. Interestingly, the process of viral membrane fusion appears to be a significant target of anti-DENV antibodies during infection in humans, with fusion loop antibodies making up a significant proportion of the population of broadly reactive antibodies that are elicited during infection with DENV (Goncalvez et al., 2004; Lai et al., 2013). Given the convergent nature of the immune response and the prevalence of the E_{315} variant, it is conceivable that the E_{315} variant arose as an immune-escape variant to fusion loop antibodies. Indeed, Goncalvez et al. (2004) demonstrated that after 11 cycles of passage in the presence of anti-fusion loop mAb 1A5, an escape mutation was isolated at E_{317} in DENV-2, further supporting our claim that immune pressures exerted by fusion loop antibodies played a key role in convergent selection for variants at the analogous E_{315} hotspot locus in DENV-3. Taken together, we conclude that the E_{315} hotspot variant, despite possibly possessing an immune-escape advantage, is constrained to the intrahost evolutionary system because of the severe defects associated with viral membrane fusion post entry.

Concluding Remarks

We have thus demonstrated that intrahost DENV-3 populations can rapidly and convergently evolve in acute human infections, with virus microevolution possibly shaped by viral replication compartments distinct from PBMCs, driven in part by immune selection pressures and constrained by replication defects at the macro-evolutionary scale. In particular, we identified a highly prevalent DENV variant (E_{315}) that likely arose as an immune-escape variant in response to pressures exerted by fusion loop antibodies, yet was constrained by severe replicative defects likely incurred due to a deficiency in viral membrane fusion with the host endosome post entry. The identification of such convergent immune pressures that appear to result in the

selection of prevalent immune-escape variants, especially ones that are constrained by replication defects or fitness costs, could be harnessed for intelligent selection of new candidates and targets for vaccine/drug design. Such snapshots of intrahost DENV diversity help to identify mechanisms driving virus microevolution in human dengue and provide new perspectives in assessing infection outcome, disease pathogenesis, and vaccine/therapeutic efficacy in individuals.

STAR★METHODS

Detailed methods are provided in the online version of this paper and include the following:

- KEY RESOURCES TABLE
- CONTACT FOR REAGENT AND RESOURCE SHARING
- EXPERIMENTAL MODEL AND SUBJECT DETAILS
  - Ethics Statement
  - Study Population
  - Cell Culture
- METHOD DETAILS
  - RNA Extraction and DENV-3 Genome Amplification
  - Consensus Genome Imputation and Variant Analysis
  - Generation of WT, $prM_{100,101}$ and E_{315} DENV-3 Viruses
  - Virus Titration
  - Relative Quantitation of Viruses by Sequencing
  - Replication in C6/36 Cells
  - Replication in U937-DC-SIGN Cells
  - RT-PCR from Serum
  - Entry Assays
- QUANTIFICATION AND STATISTICAL ANALYSIS
- DATA AND SOFTWARE AVAILABILITY

SUPPLEMENTAL INFORMATION

Supplemental Information includes five figures and four tables and can be found with this article online at http://dx.doi.org/10.1016/j.chom.2017.08.003.

AUTHOR CONTRIBUTIONS

Design of Experiments, P.P., C.W., and E.H.; Performed Experiments, S.B.T., C.W., M.E., P.P., and M.M.; Data Analysis, P.P., C.W., S.B.T., M.E., M.M., and E.H.; Resources, A.B. and E.H.; Writing – Review & Editing, P.P., C.W., and E.H.; Funding Acquisition, P.P., A.B., and E.H.

ACKNOWLEDGMENTS

This work was funded by the following grants from NIAID, NIH: R01 GM087405 to E.H., U54 AI065359 to A.B., U54 AI065359 Development Award to P.P. The content is solely the responsibility of the authors and does not necessarily represent the official views of the NIH. The authors would like to thank Shayna M. Cave, Sanjana Shah, Edwina B. Tran, and Alejandro Ramirez for technical assistance with experiments, and Dr. Andrew Fire for scientific advice. We thank members of the study team based at the Hospital Infantil Manuel de Jesús Rivera, the National Virology Laboratory in the Centro Nacional de Diagnóstico y Referencia, and the Sustainable Sciences Institute in Nicaragua for their dedication and high-quality work, as well as the children who participated in the studies and their families.

Received: April 18, 2017
Revised: July 6, 2017
Accepted: August 7, 2017
Published: September 13, 2017

REFERENCES

Aye, K.S., Charngkaew, K., Win, N., Wai, K.Z., Moe, K., Punyadee, N., Thiemmeca, S., Suttitheptumrong, A., Sukpanichnant, S., Prida, M., et al. (2014). Pathologic highlights of dengue hemorrhagic fever in 13 autopsy cases from Myanmar. Hum. Pathol. *45*, 1221–1233.

Balsitis, S.J., Coloma, J., Castro, G., Alava, A., Flores, D., McKerrow, J.H., Beatty, P.R., and Harris, E. (2009). Tropism of dengue virus in mice and humans defined by viral nonstructural protein 3-specific immunostaining. Am. J. Trop. Med. Hyg. *80*, 416–424.

Beltramello, M., Williams, K.L., Simmons, C.P., Macagno, A., Simonelli, L., Quyen, N.T., Sukupolvi-Petty, S., Navarro-Sanchez, E., Young, P.R., de Silva, A.M., et al. (2010). The human immune response to Dengue virus is dominated by highly cross-reactive antibodies endowed with neutralizing and enhancing activity. Cell Host Microbe *8*, 271–283.

Bhatt, S., Gething, P.W., Brady, O.J., Messina, J.P., Farlow, A.W., Moyes, C.L., Drake, J.M., Brownstein, J.S., Hoen, A.G., Sankoh, O., et al. (2013). The global distribution and burden of dengue. Nature *496*, 504–507.

Bull, R.A., Eden, J.S., Luciani, F., McElroy, K., Rawlinson, W.D., and White, P.A. (2012). Contribution of intra- and interhost dynamics to norovirus evolution. J. Virol. *86*, 3219–3229.

Byk, L.A., and Gamarnik, A.V. (2016). Properties and functions of the dengue virus capsid protein. Annu. Rev. Virol. *3*, 263–281.

Clyde, K., Barrera, J., and Harris, E. (2008). The capsid-coding region hairpin element (cHP) is a critical determinant of dengue virus and West Nile virus RNA synthesis. Virology *379*, 314–323.

de Alwis, R., Williams, K.L., Schmid, M.A., Lai, C.Y., Patel, B., Smith, S.A., Crowe, J.E., Wang, W.K., Harris, E., and de Silva, A.M. (2014). Dengue viruses are enhanced by distinct populations of serotype cross-reactive antibodies in human immune sera. PLoS Pathog. *10*, e1004386.

de Borba, L., Villordo, S.M., Iglesias, N.G., Filomatori, C.V., Gebhard, L.G., and Gamarnik, A.V. (2015). Overlapping local and long-range RNA-RNA interactions modulate dengue virus genome cyclization and replication. J. Virol. *89*, 3430–3437.

Debbink, K., Lindesmith, L.C., Ferris, M.T., Swanstrom, J., Beltramello, M., Corti, D., Lanzavecchia, A., and Baric, R.S. (2014). Within-host evolution results in antigenically distinct GII.4 noroviruses. J. Virol. *88*, 7244–7255.

Dejnirattisai, W., Jumnainsong, A., Onsirisakul, N., Fitton, P., Vasanawathana, S., Limpitikul, W., Puttikhunt, C., Edwards, C., Duangchinda, T., Supasa, S., et al. (2010). Cross-reacting antibodies enhance dengue virus infection in humans. Science *328*, 745–748.

Descloux, E., Cao-Lormeau, V.M., Roche, C., and De Lamballerie, X. (2009). Dengue 1 diversity and microevolution, French Polynesia 2001-2006: connection with epidemiology and clinics. PLoS Negl. Trop. Dis. *3*, e493.

Diamond, M.S., and Harris, E. (2001). Interferon inhibits dengue virus infection by preventing translation of viral RNA through a PKR-independent mechanism. Virology *289*, 297–311.

Domingo, E., and Holland, J.J. (1997). RNA virus mutations and fitness for survival. Annu. Rev. Microbiol. *51*, 151–178.

Farci, P., Strazzera, R., Alter, H.J., Farci, S., Degioannis, D., Coiana, A., Peddis, G., Usai, F., Serra, G., Chessa, L., et al. (2002). Early changes in hepatitis C viral quasispecies during interferon therapy predict the therapeutic outcome. Proc. Natl. Acad. Sci. USA *99*, 3081–3086.

Friebe, P., Shi, P.Y., and Harris, E. (2011). The 5' and 3' downstream AUG region elements are required for mosquito-borne flavivirus RNA replication. J. Virol. *85*, 1900–1905.

Gire, S.K., Goba, A., Andersen, K.G., Sealfon, R.S., Park, D.J., Kanneh, L., Jalloh, S., Momoh, M., Fullah, M., Dudas, G., et al. (2014). Genomic surveillance elucidates Ebola virus origin and transmission during the 2014 outbreak. Science *345*, 1369–1372.

Goncalvez, A.P., Purcell, R.H., and Lai, C.-J. (2004). Epitope determinants of a chimpanzee Fab antibody that efficiently cross-neutralizes dengue type 1 and type 2 viruses map to inside and in close proximity to fusion loop of the dengue type 2 virus envelope protein. J. Virol. *78*, 12919–12928.

Gutierrez, G., Gresh, L., Perez, M.A., Elizondo, D., Aviles, W., Kuan, G., Balmaseda, A., and Harris, E. (2013). Evaluation of the diagnostic utility of the traditional and revised WHO dengue case definitions. PLoS Negl. Trop. Dis. *7*, e2385.

Hall, G.S., and Little, D.P. (2007). Relative quantitation of virus population size in mixed genotype infections using sequencing chromatograms. J. Virol. Methods *146*, 22–28.

Halstead, S.B. (2009). Antibodies determine virulence in dengue. Ann. N. Y Acad. Sci. *1171* (*Suppl 1*), E48–E56.

Halstead, S.B., and Yamarat, C. (1965). Recent epidemics of hemorrhagic fever in Thailand. observations related to pathogenesis of a "new" dengue disease. Am. J. Public Health Nations Health *55*, 1386–1395.

Hammond, S.N., Balmaseda, A., Perez, L., Tellez, Y., Saborio, S.I., Mercado, J.C., Videa, E., Rodriguez, Y., Perez, M.A., Cuadra, R., et al. (2005). Differences in dengue severity in infants, children, and adults in a 3-year hospital-based study in Nicaragua. Am. J. Trop. Med. Hyg. *73*, 1063–1070.

Henchal, E.A., Gentry, M.K., McCown, J.M., and Brandt, W.E. (1982). Dengue virus-specific and flavivirus group determinants identified with monoclonal antibodies by indirect immunofluorescence. Am. J. Trop. Med. Hyg. *31*, 830–836.

Jessie, K., Fong, M.Y., Devi, S., Lam, S.K., and Wong, K.T. (2004). Localization of dengue virus in naturally infected human tissues, by immunohistochemistry and in situ hybridization. J. Infect. Dis. *189*, 1411–1418.

Johnson, B.W., Russell, B.J., and Lanciotti, R.S. (2005). Serotype-specific detection of dengue viruses in a fourplex real-time reverse transcriptase PCR assay. J. Clin. Microbiol. *43*, 4977–4983.

Joos, B., Trkola, A., Fischer, M., Kuster, H., Rusert, P., Leemann, C., Boni, J., Oxenius, A., Price, D.A., Phillips, R.E., et al. (2005). Low human immunodeficiency virus envelope diversity correlates with low in vitro replication capacity and predicts spontaneous control of plasma viremia after treatment interruptions. J. Virol. *79*, 9026–9037.

Lai, C.Y., Williams, K.L., Wu, Y.C., Knight, S., Balmaseda, A., Harris, E., and Wang, W.K. (2013). Analysis of cross-reactive antibodies recognizing the fusion loop of envelope protein and correlation with neutralizing antibody titers in Nicaraguan dengue cases. PLoS Negl. Trop. Dis. *7*, e2451.

Langmead, B., and Salzberg, S.L. (2012). Fast gapped-read alignment with Bowtie 2. Nat. Methods *9*, 357–359.

Lee, H.Y., Perelson, A.S., Park, S.C., and Leitner, T. (2008). Dynamic correlation between intrahost HIV-1 quasispecies evolution and disease progression. PLoS Comput. Biol. *4*, e1000240.

Li, H., Handsaker, B., Wysoker, A., Fennell, T., Ruan, J., Homer, N., Marth, G., Abecasis, G., Durbin, R., and Genome Project Data Processing, S. (2009). The sequence alignment/map format and SAMtools. Bioinformatics *25*, 2078–2079.

Lin, S.R., Hsieh, S.C., Yueh, Y.Y., Lin, T.H., Chao, D.Y., Chen, W.J., King, C.C., and Wang, W.K. (2004). Study of sequence variation of dengue type 3 virus in naturally infected mosquitoes and human hosts: implications for transmission and evolution. J. Virol. *78*, 12717–12721.

Messer, W.B., Gubler, D.J., Harris, E., Sivananthan, K., and de Silva, A.M. (2003). Emergence and global spread of a dengue serotype 3, subtype III virus. Emerg. Infect. Dis. *9*, 800–809.

Messer, W.B., Yount, B., Hacker, K.E., Donaldson, E.F., Huynh, J.P., de Silva, A.M., and Baric, R.S. (2012). Development and characterization of a reverse genetic system for studying dengue virus serotype 3 strain variation and neutralization. PLoS Negl. Trop. Dis. *6*, e1486.

Moreau, I., Levis, J., Crosbie, O., Kenny-Walsh, E., and Fanning, L.J. (2008). Correlation between pre-treatment quasispecies complexity and treatment outcome in chronic HCV genotype 3a. Virol. J. *5*, 78.

Narvaez, F., Gutierrez, G., Perez, M.A., Elizondo, D., Nunez, A., Balmaseda, A., and Harris, E. (2011). Evaluation of the traditional and revised WHO classifications of Dengue disease severity. PLoS Negl. Trop. Dis. *5*, e1397.

Nelson, S., Poddar, S., Lin, T.Y., and Pierson, T.C. (2009). Protonation of individual histidine residues is not required for the pH-dependent entry of West Nile virus: evaluation of the "histidine switch" hypothesis. J. Virol. *83*, 12631–12635.

Nguyen, T.P., Kikuchi, M., Vu, T.Q., Do, Q.H., Tran, T.T., Vo, D.T., Ha, M.T., Vo, V.T., Cao, T.P., Tran, V.D., et al. (2008). Protective and enhancing HLA alleles, HLA-DRB1*0901 and HLA-A*24, for severe forms of dengue virus infection, dengue hemorrhagic fever and dengue shock syndrome. PLoS Negl. Trop. Dis. *2*, e304.

Ni, M., Chen, C., Qian, J., Xiao, H.X., Shi, W.F., Luo, Y., Wang, H.Y., Li, Z., Wu, J., Xu, P.S., et al. (2016). Intra-host dynamics of Ebola virus during 2014. Nat. Microbiol. *1*, 16151.

OhAinle, M., Balmaseda, A., Macalalad, A.R., Tellez, Y., Zody, M.C., Saborio, S., Nunez, A., Lennon, N.J., Birren, B.W., Gordon, A., et al. (2011). Dynamics of dengue disease severity determined by the interplay between viral genetics and serotype-specific immunity. Sci. Transl. Med. *3*, 114ra128.

Parameswaran, P., Charlebois, P., Tellez, Y., Nunez, A., Ryan, E.M., Malboeuf, C.M., Levin, J.Z., Lennon, N.J., Balmaseda, A., Harris, E., et al. (2012). Genome-wide patterns of intrahuman dengue virus diversity reveal associations with viral phylogenetic clade and interhost diversity. J. Virol. *86*, 8546–8558.

Park, D., Huh, H.J., Kim, Y.J., Son, D.S., Jeon, H.J., Im, E.H., Kim, J.W., Lee, N.Y., Kang, E.S., Kang, C.I., et al. (2016). Analysis of intrapatient heterogeneity uncovers the microevolution of Middle East respiratory syndrome coronavirus. Cold Spring Harb. Mol. Case Stud. *2*, a001214.

Peiris, J.S., and Porterfield, J.S. (1979). Antibody-mediated enhancement of Flavivirus replication in macrophage-like cell lines. Nature *282*, 509–511.

Quiner, C.A., Parameswaran, P., Ciota, A.T., Ehrbar, D.J., Dodson, B.L., Schlesinger, S., Kramer, L.D., and Harris, E. (2014). Increased replicative fitness of a dengue virus 2 clade in native mosquitoes: potential contribution to a clade replacement event in Nicaragua. J. Virol. *88*, 13125–13134.

Rico-Hesse, R., Harrison, L.M., Salas, R.A., Tovar, D., Nisalak, A., Ramos, C., Boshell, J., de Mesa, M.T., Nogueira, R.M., and da Rosa, A.T. (1997). Origins of dengue type 2 viruses associated with increased pathogenicity in the Americas. Virology *230*, 244–251.

Rivino, L., Kumaran, E.A., Jovanovic, V., Nadua, K., Teo, E.W., Pang, S.W., Teo, G.H., Gan, V.C., Lye, D.C., Leo, Y.S., et al. (2013). Differential targeting of viral components by CD4+ versus CD8+ T lymphocytes in dengue virus infection. J. Virol. *87*, 2693–2706.

Rodriguez-Roche, R., Blanc, H., Borderia, A.V., Diaz, G., Henningsson, R., Gonzalez, D., Santana, E., Alvarez, M., Castro, O., Fontes, M., et al. (2016). Increasing clinical severity during a dengue virus type 3 Cuban epidemic: deep sequencing of evolving viral populations. J. Virol. *90*, 4320–4333.

Rogers, M.B., Song, T., Sebra, R., Greenbaum, B.D., Hamelin, M.E., Fitch, A., Twaddle, A., Cui, L., Holmes, E.C., Boivin, G., et al. (2015). Intrahost dynamics of antiviral resistance in influenza a virus reflect complex patterns of segment linkage, reassortment, and natural selection. MBio *6*, e02464-14.

Rothman, A.L., and Ennis, F.A. (1999). Immunopathogenesis of Dengue hemorrhagic fever. Virology *257*, 1–6.

Selisko, B., Wang, C., Harris, E., and Canard, B. (2014). Regulation of flavivirus RNA synthesis and replication. Curr. Opin. Virol. *9*, 74–83.

Sessions, O.M., Wilm, A., Kamaraj, U.S., Choy, M.M., Chow, A., Chong, Y., Ong, X.M., Nagarajan, N., Cook, A.R., and Ooi, E.E. (2015). Analysis of dengue virus genetic diversity during human and mosquito infection reveals genetic constraints. PLoS Negl. Trop. Dis. *9*, e0004044.

Sim, S., Aw, P.P., Wilm, A., Teoh, G., Hue, K.D., Nguyen, N.M., Nagarajan, N., Simmons, C.P., and Hibberd, M.L. (2015). Tracking dengue virus intra-host genetic diversity during human-to-mosquito transmission. PLoS Negl. Trop. Dis. *9*, e0004052.

Simmons, C.P., Dong, T., Chau, N.V., Dung, N.T., Chau, T.N., Thao le, T.T., Dung, N.T., Hien, T.T., Rowland-Jones, S., and Farrar, J. (2005). Early T-cell responses to dengue virus epitopes in Vietnamese adults with secondary dengue virus infections. J. Virol. *79*, 5665–5675.

Sobel Leonard, A., McClain, M.T., Smith, G.J., Wentworth, D.E., Halpin, R.A., Lin, X., Ransier, A., Stockwell, T.B., Das, S.R., Gilbert, A.S., et al. (2016). Deep sequencing of influenza a virus from a human challenge study reveals

a selective bottleneck and only limited intrahost genetic diversification. J. Virol. *90*, 11247–11258.

Stapleford, K.A., Moratorio, G., Henningsson, R., Chen, R., Matheus, S., Enfissi, A., Weissglas-Volkov, D., Isakov, O., Blanc, H., Mounce, B.C., et al. (2016). Whole-genome sequencing analysis from the chikungunya virus Caribbean outbreak reveals novel evolutionary genomic elements. PLoS Negl. Trop. Dis. *10*, e0004402.

Sullivan, D.G., Bruden, D., Deubner, H., McArdle, S., Chung, M., Christensen, C., Hennessy, T., Homan, C., Williams, J., McMahon, B.J., et al. (2007). Hepatitis C virus dynamics during natural infection are associated with long-term histological outcome of chronic hepatitis C disease. J. Infect. Dis. *196*, 239–248.

Tassaneetrithep, B., Burgess, T.H., Granelli-Piperno, A., Trumpfheller, C., Finke, J., Sun, W., Eller, M.A., Pattanapanyasat, K., Sarasombath, S., Birx, D.L., et al. (2003). DC-SIGN (CD209) mediates dengue virus infection of human dendritic cells. J. Exp. Med. *197*, 823–829.

Thai, K.T., Henn, M.R., Zody, M.C., Tricou, V., Nguyet, N.M., Charlebois, P., Lennon, N.J., Green, L., de Vries, P.J., Hien, T.T., et al. (2012). High-resolution analysis of intrahost genetic diversity in dengue virus serotype 1 infection identifies mixed infections. J. Virol. *86*, 835–843.

Valkenburg, S.A., Quinones-Parra, S., Gras, S., Komadina, N., McVernon, J., Wang, Z., Halim, H., Iannello, P., Cole, C., Laurie, K., et al. (2013). Acute emergence and reversion of influenza A virus quasispecies within CD8+ T cell antigenic peptides. Nat. Commun. *4*, 2663.

Wang, W.K., Lin, S.R., Lee, C.M., King, C.C., and Chang, S.C. (2002a). Dengue type 3 virus in plasma is a population of closely related genomes: quasispecies. J. Virol. *76*, 4662–4665.

Wang, W.K., Sung, T.L., Lee, C.N., Lin, T.Y., and King, C.C. (2002b). Sequence diversity of the capsid gene and the nonstructural gene NS2B of dengue-3 virus in vivo. Virology *303*, 181–191.

Weiskopf, D., Angelo, M.A., de Azeredo, E.L., Sidney, J., Greenbaum, J.A., Fernando, A.N., Broadwater, A., Kolla, R.V., De Silva, A.D., de Silva, A.M., et al. (2013). Comprehensive analysis of dengue virus-specific responses supports an HLA-linked protective role for CD8+ T cells. Proc. Natl. Acad. Sci. USA *110*, E2046–E2053.

WHO. (1997). Dengue Haemorrhagic Fever: Diagnosis, Treatment, Prevention and Control, Second Edition (WHO).

Zagordi, O., Bhattacharya, A., Eriksson, N., and Beerenwinkel, N. (2011). ShoRAH: estimating the genetic diversity of a mixed sample from next-generation sequencing data. BMC Bioinformatics *12*, 119.

Zheng, A., Yuan, F., Kleinfelter, L.M., and Kielian, M. (2014). A toggle switch controls the low pH-triggered rearrangement and maturation of the dengue virus envelope proteins. Nat. Commun. *5*, 3877.

STAR★METHODS

KEY RESOURCES TABLE

REAGENT or RESOURCE	SOURCE	IDENTIFIER
Antibodies		
anti-E (5D4)	Hybridoma from ATCC	5D4-11 (ATCC® HB-49™), RRID: CVCL_J928; Henchal et al. (1982)
anti-NS3 (E1D8)	Hybridoma generated in Harris Laboratory	E1D8, Balsitis et al. (2009)
Bacterial and Virus Strains		
E. coli TOP10 competent cells	Invitrogen	C4040-10
Biological Samples		
PBMC and plasma samples	This paper: Table S1	N/A
Chemicals, Peptides, and Recombinant Proteins		
Kanamycin Sulfate	Life Technologies	11815-024
Chloramphenicol >=98% (TLC)	Sigma-Aldrich	C0378-25G
Critical Commercial Assays		
RNeasy Mini kit	Qiagen	Cat No./ID: 74104
QIAamp Viral RNA Mini Kit	Qiagen	Cat No./ID: 52904
QIAquick Gel Extraction Kit	Qiagen	Cat No./ID: 28704
Nextera XT DNA Sample Preparation Kit	Illumina	FC-131-1096
SuperScript III One-Step RT-PCR System	Invitrogen	12574-035
mMessage mMachine T7 Kit	Life Technology	AM1344M
MinElute Gel Extraction Kit (50) (70bp to 4kb)	Qiagen	Qia 28604
Deposited Data		
Fastq files for all these samples have been deposited into	NCBI's Sequence Read Archive	BioProject ID PRJNA394021
Experimental Models: Cell Lines		
Baby hamster kidney cells (BHK-21 clone 15)	Gift from B. Childs (Center for Vector-born Diseases, University of California, Davis, CA)	N/A
C6/36 cells, 37°C in 5% CO_2.	Gift from Dr. Ralph Baric, University of North Carolina, Chapel Hill	N/A
U937-DC-SIGN cells	Gift of Dr. Aravinda de Silva, University of North Carolina, Chapel Hill	N/A
Oligonucleotides		
Sequences of primers used for amplifying the DENV-3 genome	Table S4 of this paper	N/A
DV3Ewt_r: CGACCTTAATGAGTATTGTCCCAT	This paper	N/A
DV3E*_r: CGACCTTAATGAGTATTGTCCCAa	This paper	N/A
PP49_DENV3_32_F (GACTCGGAAGCTTGCTTAAC)	This paper	N/A
primers (5'- GACTCGGAAGCTTGCTTAAC-3' and 5'-TATTGACAGGCTCCTCCTTCTTAG-3') designed to capture the $prM_{100,101}$ and E_{315} hotspot loci	This paper	N/A
Sequencing primer for $prM_{100,101}$: 5'-TCAATATGC TGAAACGCGTG-3'	This paper	N/A
Sequencing primer for E_{315}: 5'-CGGACAGGTTT GGATTTCAATG-3'	This paper	N/A
Recombinant DNA		
plasmid A-D	Gift of Dr. Ralph Baric	Messer et al., 2012
plasmid A Nicaraguan WT	This paper	N/A

(*Continued on next page*)

Continued

REAGENT or RESOURCE	SOURCE	IDENTIFIER
plasmid A Nicaraguan $prM_{100,101}$	This paper	N/A
plasmid A Nicaraguan E_{315}	This paper	N/A
Software and Algorithms		
Bowtie2	Langmead and Salzberg, 2012	http://bowtie-bio.sourceforge.net/bowtie2/index.shtml
Samtools	Li et al., 2009	http://samtools.sourceforge.net/
ShoRAH	Zagordi et al., 2011	http://www.cbg.ethz.ch/software/shorah

CONTACT FOR REAGENT AND RESOURCE SHARING

Further information and requests for resources and reagents should be directed to and will be fulfilled by the Lead Contact, Dr. Eva Harris (eharris@berkeley.edu).

EXPERIMENTAL MODEL AND SUBJECT DETAILS

Ethics Statement

All studies were approved by the Institutional Review Boards (IRBs) of the University of California, Berkeley, and of the Nicaraguan Ministry of Health. Written consent was obtained from the parents/legal guardians of all pediatric subjects. Assent was also obtained from subjects six years of age or older.

Study Population

PBMC and plasma samples were obtained from subjects in an ongoing prospective hospital-based study of pediatric dengue in Nicaragua established in 1998 (Hammond et al., 2005), which enrolls patients who present with suspected dengue to the National Pediatric Reference Hospital in Managua, Nicaragua. Plasma and PBMCs are collected from patients for three sequential days during the acute phase of illness, at convalescence (days 14-28) and longitudinally for 18 months. Criteria for identifying dengue-positive cases and for classifying by immune status are as described (Gutierrez et al., 2013; Narvaez et al., 2011). Dengue cases are classified as DF, DHF, or DSS according to the 1997 WHO Dengue Guidelines (Narvaez et al., 2011; WHO, 1997). Thirty-one plasma and 68 peripheral blood mononuclear cell (PBMC) samples from 77 individuals (including 22 with paired plasma and PBMC samples) were analyzed in this study. The gender identity as well as the age of the patients is listed in Table S1. Extensive epidemiological and clinical data are available for these samples. The sample size for this study was determined by availability of pediatric patient samples for primary and secondary dengue cases caused by DENV-3 within a single endemic year (2009-2010). Subgroups within the 77 patients in the study were selected based on sample type (plasma versus PBMCs), clinical classification (for example, primary versus secondary dengue, Dengue Fever versus Dengue Hemorrhagic Fever and Dengue Shock Syndrome), or gene origin of variation (based on DENV-3 gene annotation).

Cell Culture

Baby hamster kidney cells (BHK-21 clone 15) were maintained in αMEM (Gibco) supplemented with 5% heat-inactivated Fetal Bovine Serum (FBS; Gibco), 10 mM HEPES (Gibco), and 100 U/ml penicillin and 100 μg/ml streptomycin (Pen/Strep; Gibco) at 37°C in 5% CO_2. C6/36 cells (gift of Dr. Ralph Baric) were maintained in MEM with HEPES supplemented with 10% heat-inactivated FBS, 1X non-essential amino acids (NEAA; Gibco), 2 mM L-glutamine (Gibco) and Pen/Strep at 32°C in 5% CO_2. U937 cells expressing DC-SIGN (U937-DC-SIGN, gift of Dr. Aravinda de Silva) were maintained in RPMI 1640 medium (Gibco) supplemented with 5% FBS, 1% Pen/Strep and 1% HEPES at 37°C in 5% CO_2.

METHOD DETAILS

RNA Extraction and DENV-3 Genome Amplification

A hybrid TRIzol/RNeasy protocol was developed for viral RNA recovery from PBMCs. Briefly, PBMCs were lysed in TRIzol (Life Technologies), and aqueous phase RNA was extracted after addition of chloroform. Next, 3.5 volumes of Buffer RLT (RNeasy Mini kit; Qiagen) and 2.5 volumes of 100% ethanol were added to the RNA solution, and the mixture was applied to an RNeasy column. All washes and RNA elutions were performed as described (RNeasy kit protocol). Viral RNA from plasma samples was extracted using the QIAamp Viral RNA Mini Kit (Qiagen) as described in the manufacturer's protocol. RNA was eluted in 50 μl of RNase-free water containing linear polyacrylamide (1 μl; Life Technologies), carrier RNA (0.1 μl; Qiagen), and SUPERase-In (1 μl; Life Technologies). Twelve RT/PCR amplifications were set up for each sample, with various combinations of forward and reverse primers (Table S4) and reagents from the SuperScript III One-Step RT-PCR System (Invitrogen). For each reaction, we used 5 ul

of denatured RNA, 17.5 ul of a 2X reaction mix, 0.25 ul each of forward and reverse primers (100 uM), 0.7ul of the enzyme mix, and 11.3 ul of RNase-free water. DENV-3 RNA was reverse-transcribed (50°C for 60 minutes) and cDNA was amplified as follows: 1 cycle of denaturation (94°C for 2 minutes), 35 cycles of denaturation (94°C for 15 seconds), annealing (55°C for 30 seconds), and extension (68°C for 3 minutes), and a final extension step (68°C for 10 minutes)}. The conditions were identical for all amplicons except amplicon 4, for which the extension time was shortened to 1 minute. DENV-3 amplicons were purified on a 1% agarose gel, and DNA was recovered using the QIAquick Gel Extraction Kit (Qiagen). For each sample, PCR amplicons were pooled in equimolar ratios, and indexed libraries were prepared for high-throughput sequencing using the Nextera XT DNA Sample Preparation Kit (Illumina). Nextera XT libraries were pooled and sequenced for 150 cycles in two lanes on Illumina's HiSeq 2000 platform to generate paired-end datasets.

Consensus Genome Imputation and Variant Analysis

Reads were segregated based on their forward (read 1) and reverse (read 2) indices. The paired-end datasets for reads 1 and 2 were analyzed separately for all samples.

Filtering for Read Quality

The Fastx toolkit (http://hannonlab.cshl.edu/fastx_toolkit/) was used to (a) trim reads with low quality (<Q30) at the 3' end, (b) remove reads less than 50 nucleotides in length, and (c) only retain reads of high quality sequence ($\geq$Q30) at $\geq$90% of read length.

Read Alignments and Variant Identification

We generated a DENV-3 consensus genome based on all sequenced Nicaraguan DENV-3 isolates from the 2009-2010 epidemic year (n = 108; NCBI Virus Variation Database). Read 1 and read 2 datasets for each sample were aligned to the Nicaraguan DENV-3 consensus genome using *Bowtie2* (Langmead and Salzberg, 2012). *SAMtools* (Li et al., 2009) was used to create a pileup file from the *Bowtie2* output, and pileup files were filtered based on a minimum read quality score of 30 and minimum coverage of 5 reads. Consensus genomes were created for each dataset using in-house scripts, and gaps were filled with Nicaraguan DENV-3 consensus sequences. All datasets were re-aligned to their corresponding consensus genomes using *Bowtie2,* and pileup files generated by *SAMtools* were filtered based on quality scores ($\geq$30). Fastq files for all the sequences generated in this study have been deposited into NCBI's Sequence Read Archive, and can be accessed using BioProject ID PRJNA394021. In-house scripts were used to calculate percent variant abundance in nucleotide, codon and amino acid coordinates at all loci with a minimum coverage of 5 reads.

Threshold for Variant Abundance

Replicate amplicon libraries were analyzed in a pairwise manner to set abundance thresholds for high-confidence variant detection. In replicate amplicon libraries from four PBMC samples, all variants that were detected at an abundance of $\geq$0.5% in replicate A were also detected in replicate B (Figure S1B, *left panels*) and *vice versa* (*data not shown*). However, the threshold for variant detection in both replicates was considerably higher for replicate libraries from the three serum samples ($\geq$1.0%; Figure S1B, *right panels*). Additionally, frequency distribution of loci by percent variant abundance in replicate B, for various thresholds of percent variant abundances in replicate A, revealed that concordance of 50% or higher between replicates was achieved at loci with $\geq$1.0% variant abundance in both PBMC and serum samples (Figure S1C, *left and right panels*, respectively). For identifying variants, we implemented the following thresholds: (a) loci should have a minimum coverage of 1000 reads, (b) variant abundance must be $\geq$1%, and (c) variant cannot be in a primer-binding region.

Reconstructing Haplotypes

The software package *ShoRAH* (Zagordi et al., 2011) was used to reconstruct 150 nucleotide-haplotypes spanning the $prM_{100,101}$ and E_{315} hotspot loci. Only haplotypes with a reconstruction quality score of $\geq$0.9 were considered for diversity analysis.

Generation of WT, $prM_{100,101}$ and E_{315} DENV-3 Viruses

A four-plasmid infectious clone system (plasmids A-D; gift of Dr. Ralph Baric (Messer et al., 2012)) based on a Sri Lankan DENV-3 template was used to derive Nicaraguan WT DENV-3 and DENV-3 with mutations at the $prM_{100,101}$ or E_{315} hotspot loci. We introduced four amino acid changes in the C, prM and E sequences in plasmid A (P27S, I286V, V361T and A609V in the DENV-3 polyprotein) to generate infectious clones that were identical in structural protein sequence to the Nicaraguan DENV-3 consensus genome ("WT"). The $prM_{100,101}$ mutations were inserted by site-directed mutagenesis in plasmid A using the QuikChange site-directed mutagenesis kit (Stratagene). The E_{315} mutation was synthesized in the context of a plasmid A fragment spanning nucleotides 1-2034 of the DENV-3 genome (Bio Basic, Inc.). Infectious clones for WT, $prM_{100,101}$ and E_{315} viruses were derived as described (Messer et al., 2012), with some modifications. All plasmids were individually propagated in *E. coli* TOP10 competent cells (Invitrogen) and grown on LB plates with selective antibiotics (plasmid A encoding for WT, $prM_{100,101}$ and E_{315} was selected with ampicillin, plasmids B and C with kanamycin, and plasmid D with chloramphenicol) at 30°C for 24 hours. Sequences of colony-purified plasmids were confirmed by Sanger sequencing, and restriction digests were set up as follows: plasmid A with SpeI, AhdI and BsmBI yielding a 2.0-kb fragment; plasmid B with BglI and BsmBI yielding a 1.1-kb fragment; plasmid C with BglI yielding a 3.9-kb fragment; and plasmid D with BglI and BsmbI yielding a 3.0-kb fragment. Fragments were gel-purified using a MinElute Gel Extraction Kit (Qiagen), mixed in equimolar ratios, and ligated with T4 ligase (NEB) for 2 hours at 16°C. Full-length transcripts of DENV-3 cDNA constructs were generated *in vitro* as described using the mMessage mMachine T7 Kit (Ambion) with the following modifications: (a) 20 μl reaction mixtures were supplemented with 2 μl of a 30 mM GTP stock, resulting in a 1.3:1 ratio of cap analog to GTP, and (b) the reaction was incubated at 37°C for 3 hours. For electroporation, DENV-3 transcripts were added to 400 μl of BHK cell suspension (1 x 10^7 cells/ml in RNase-free PBS) in an electroporation cuvette, and pulsed once with 270 V (975 μF) in a Bio-Rad

Gene Pulser II electroporator. The transfected BHK cells were grown in a 75 cm^2 flask and incubated at 37°C for 5 days. For virus amplification, 2 ml of viral supernatant from BHK cells was used to infect C6/36 cells in a 75 cm^2 flask, and 18 ml of C6/36 media (1X MEM + 2% FBS + 1% Pen/Strep + 1% NEAA + 1% L-Glutamine) was added to the cells. Supernatants were harvested five days post-infection, supplemented to 1X SPG (sucrose-phosphate-glutamate stabilizer, prepared in-house), clarified by centrifugation, and frozen at −80°C or passaged serially in C6/36 cells.

Virus Titration

For plaque assays, ten-fold serial dilutions of virus culture supernatant (undiluted, and dilutions of 10^{-1} to 10^{-5}) were added in duplicate to cultured BHK-21 cells in 24-well plates and incubated for 1 h at 37°C. After discarding the inoculum, the cells were overlaid with 1 ml of 0.8% carboxymethyl cellulose in MEM supplemented with 2% FBS and Pen/Strep. Plates were incubated for 4 days at 37°C in 5% CO_2. Overlays were removed, cells were fixed with formalin and stained with 2.5% crystal violet in 30% ethanol, and plaque-forming units per ml (PFU/ml) were counted. For assaying temperature sensitivity, infections and post-infection incubations were performed at 32°C in 5% CO_2, and plaques were counted 7 days p.i.. For quantitative RT-PCR (qRT-PCR), 18 μl-reactions were set up with 2 μl RNA, DENV-3 specific primers (Johnson et al., 2005), 0.1 μM DENV-3 probe (Johnson et al., 2005), and reagents from the Verso 1-Step qRT-PCR kit (Thermo Scientific). Reaction conditions were as follows: 1 cycle of reverse transcription (30 minutes at 50°C), 1 cycle of Thermo-Start activation (12.5 minutes at 95°C), and 40 cycles of denaturation (15 seconds at 95°C) and annealing/extension (1 minute at 60°C). A standard curve was used to calculate DENV-3 genome equivalents per ml (GE/ml) for each test sample.

Relative Quantitation of Viruses by Sequencing

Viral RNA was amplified using reagents from the SuperScript III One-Step RT-PCR System, with primers (5'- GACTCGGAA GCTTGCTTAAC-3' and 5'-TATTGACAGGCTCCTCCTTCTTAG-3') designed to capture the $prM_{100,101}$ and E_{315} hotspot loci. Amplicons were gel-purified and sequenced by the Sanger method using primers 5'-TCAATATGCTGAAACGCGTG-3' and 5'-CGGACA GGTTTGGATTTCAATG-3' for capturing chromatogram peak heights at the $prM_{100,101}$ and E_{315} loci, respectively. Relative levels of WT and mutant viruses were calculated from quantitation of chromatogram peak heights at the hotspot loci corresponding to WT and mutant nucleotides using the PolySNP program (Hall and Little, 2007).

Replication in C6/36 Cells

For each infection, we used six-well plates with 2 X 10^5 C6/36 cells per well, and a virus mix containing 1000 GE/cell of WT and 1000 GE/cell of $prM_{100,101}$ or E_{315} viruses (as determined by qRT-PCR) diluted in Hank's Balanced Salt Solution (HBSS; Gibco). One hundred μl of the virus mix was stored for assessing input ratios. C6/36 cells were infected with each virus mix for 2 h at 32°C in 5% CO_2, washed with PBS, and incubated in MEM containing 2% FBS, 1% Pen/Strep, 1% NEAA and 1% L-Glutamine. Supernatants were collected from independent wells at 3, 4 and 5 d.p.i.. Viral RNA was extracted from supernatants and the input virus mix using the QIAamp Viral RNA kit (Qiagen). All experiments were performed in duplicate. Relative levels of WT and mutant viruses were estimated using Sanger sequencing and the polySNP program (Hall and Little, 2007).

Replication in U937-DC-SIGN Cells

Infections were set up in 96-well plates with 5 x 10^4 U937-DC-SIGN cells per well. Infections were performed with 625 GE/cell of WT, $prM_{100,101}$ or E_{315} viruses, diluted in HBSS. Cells were infected with each virus mix for 2 h at 37°C in 5% CO_2, washed and incubated in medium containing RPMI 1640, 2% FBS, 1% Pen/Strep and 1% HEPES for 24, 48 or 72 h at 37°C in 5% CO_2. Cells were stained at room temperature with a 1:500 dilution of Zombie Aqua stain (BioLegend), fixed, permeabilized, and stained with a 1:250 dilution of an anti-E (5D4) (Henchal et al., 1982) monoclonal antibody conjugated to Texas Red and a 1:500 dilution of an anti-NS3 (E1D8) (Balsitis et al., 2009) monoclonal antibody conjugated to APC. All experiments were performed in duplicate. The percent of infected cells was measured via flow cytometry on an LSR Fortessa cell analyzer (BD Biosciences), and the data were analyzed using FlowJo 8.8.7 software (TreeStar).

RT-PCR from Serum

Reverse primers specific for WT or E_{315} mutant virus were designed as follows: primer WT (DV3Ewt_r: CGACCTTAATGAG TATTGTCCCAT); primer E_{315} (DV3E*_r: CGACCTTAATGAGTATTGTCCCAa). In combination with the forward primer PP49_DENV3_32_F (GACTCGGAAGCTTGCTTAAC), both primer sets generated an RT-PCR amplicon of 1,865bp. RT-PCR was carried out using SuperScript® III One-Step RT-PCR System with Platinum® Taq High Fidelity (Invitrogen). The RT-PCR products were visualized using an agarose gel (1%).

Entry Assays

The entry assay was performed as previously described (Diamond and Harris, 2001) with slight modifications. Specifically, 10μl of U937-DC-SIGN cells (1x10^7 cells/ml, total of 1x10^5 cells) was aliquoted into microcentrifuge tubes in triplicate, mixed with WT virus (multiplicity of infection of 0.5), E_{315} variant virus or $prM_{100,101}$ variant virus diluted in 240μl of U937-DC-SIGN culture medium, and incubated at 37°C for 2 hours with occasional agitation to avoid pelleting. All samples were then iced and washed three times with

500μl of U937-DC-SIGN culture medium at 4°C, and washed twice with 500μl PBS at 4°C. Then 350μl of lysis buffer was added to cell pellets, and RNA extraction was performed using RNeasy Mini Kit (QIAGEN). qRT-PCR was performed as described above.

QUANTIFICATION AND STATISTICAL ANALYSIS

Different statistical analyses were performed and are specified in the corresponding results in the main text or in figure legends when describing the analysis, such as Fisher's exact test (Figure 2C, main text), Wilcoxon test for unpaired samples (Figure 1B, figure legend), Wilcoxon signed-rank test (Figures 1A, 1D, and 1E, figure legend), Wilcoxon signed-rank test for paired samples (Figure 1F, figure legend). Significance was generally defined as $^{*}P \leq 0.01$, $^{**}P \leq 0.001$, while $P < 0.0001$ was also indicated where applicable. The number of samples (*n*) used for all comparisons is indicated in the figure legends as well as in the main text. Briefly, samples from 53 individuals with 1° and 46 individuals with 2° dengue were used for comparisons presented in Figures 1A–1C. Samples from 22 paired PBMC and plasma samples were used in Figures 1D and 1E. Samples from 12 paired PBMC and plasma samples were used in Figure 1F. Samples from 68 PBMC and 31 plasma samples were used in Figures 2A–2D. In Figure 2E, 690 full-length DENV-3 genomes were analyzed. Data from 8 PBMC/plasma samples (*prM/M* hotspot) and 39 PBMC/plasma samples (*E* hotspot) are shown in Figure 3. Data from 2 independent experiments were used in Figure 4.

DATA AND SOFTWARE AVAILABILITY

Fastq files for all the sequences generated in this study have been deposited into NCBI's Sequence Read Archive, and can be accessed using BioProject ID PRJNA394021.

Cell Host & Microbe, Volume *22*

Supplemental Information

Intrahost Selection Pressures Drive Rapid Dengue Virus Microevolution in Acute Human Infections

Poornima Parameswaran, Chunling Wang, Surbhi Bharat Trivedi, Meghana Eswarappa, Magelda Montoya, Angel Balmaseda, and Eva Harris

Title

Intrahost selection pressures drive rapid dengue virus microevolution in acute human infections

Authors

Poornima Parameswaran[1,3], Chunling Wang[1,3], Surbhi Bharat Trivedi[1], Meghana Eswarappa[1], Magelda Montoya[1], Angel Balmaseda[2] and Eva Harris[1,4,*]

Author affiliations

[1]Division of Infectious Diseases and Vaccinology, School of Public Health, University of California, Berkeley, Berkeley, CA, 94720-3370 USA

[2]Laboratorio Nacional de Virología, Centro Nacional de Diagnóstico y Referencia, Ministry of Health, Managua, 16064 Nicaragua

[3]These authors contributed equally

[4]Lead Contact

[*]Corresponding author: Dr. Eva Harris, Division of Infectious Diseases and Vaccinology, School of Public Health, University of California, Berkeley, 185 Li Ka Shing Center, 1951 Oxford Street, Berkeley, CA, 94720-3370, USA; Tel. 510-642-4845; FAX 510-642-6350; Email: eharris@berkeley.edu

Running Title

Intrahost virus microevolution in human dengue

Figure S1

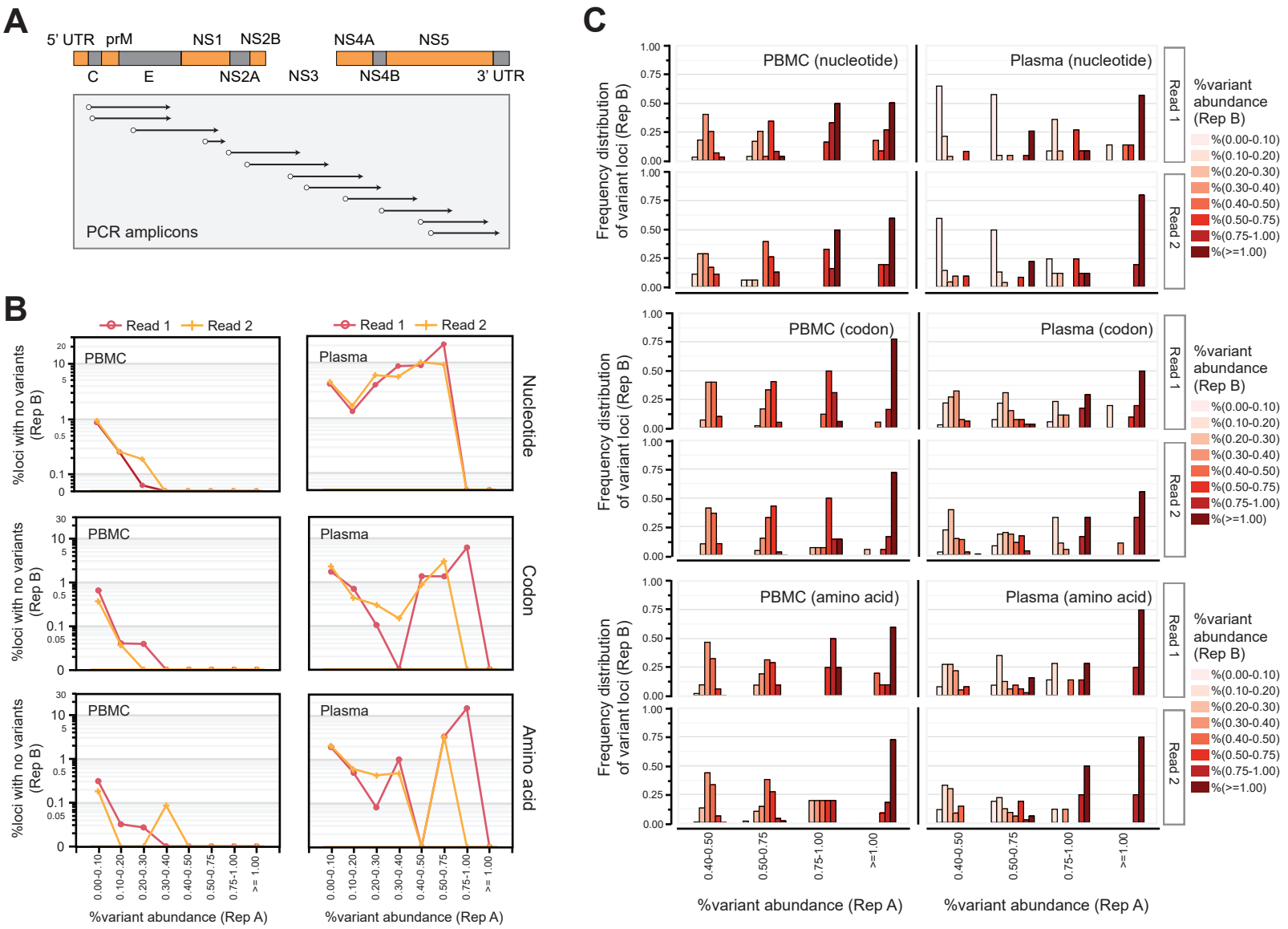
A
5' UTR
prM
NS1
NS2B
NS4A
NS5
C
E
NS2A
NS3
NS4B
3' UTR
PCR amplicons
B
Read 1
Read 2
PBMC
Plasma
Nucleotide
Codon
Amino acid
%loci with no variants (Rep B)
0.00-0.10
0.10-0.20
0.20-0.30
0.30-0.40
0.40-0.50
0.50-0.75
0.75-1.00
>= 1.00
%variant abundance (Rep A)
C
PBMC (nucleotide)
Plasma (nucleotide)
PBMC (codon)
Plasma (codon)
PBMC (amino acid)
Plasma (amino acid)
Frequency distribution of variant loci (Rep B)
Read 1
Read 2
%variant abundance (Rep B)
%(0.00-0.10)
%(0.10-0.20)
%(0.20-0.30)
%(0.30-0.40)
%(0.40-0.50)
%(0.50-0.75)
%(0.75-1.00)
%(>=1.00)
0.40-0.50
0.50-0.75
0.75-1.00
>=1.00
%variant abundance (Rep A)

Figure S2

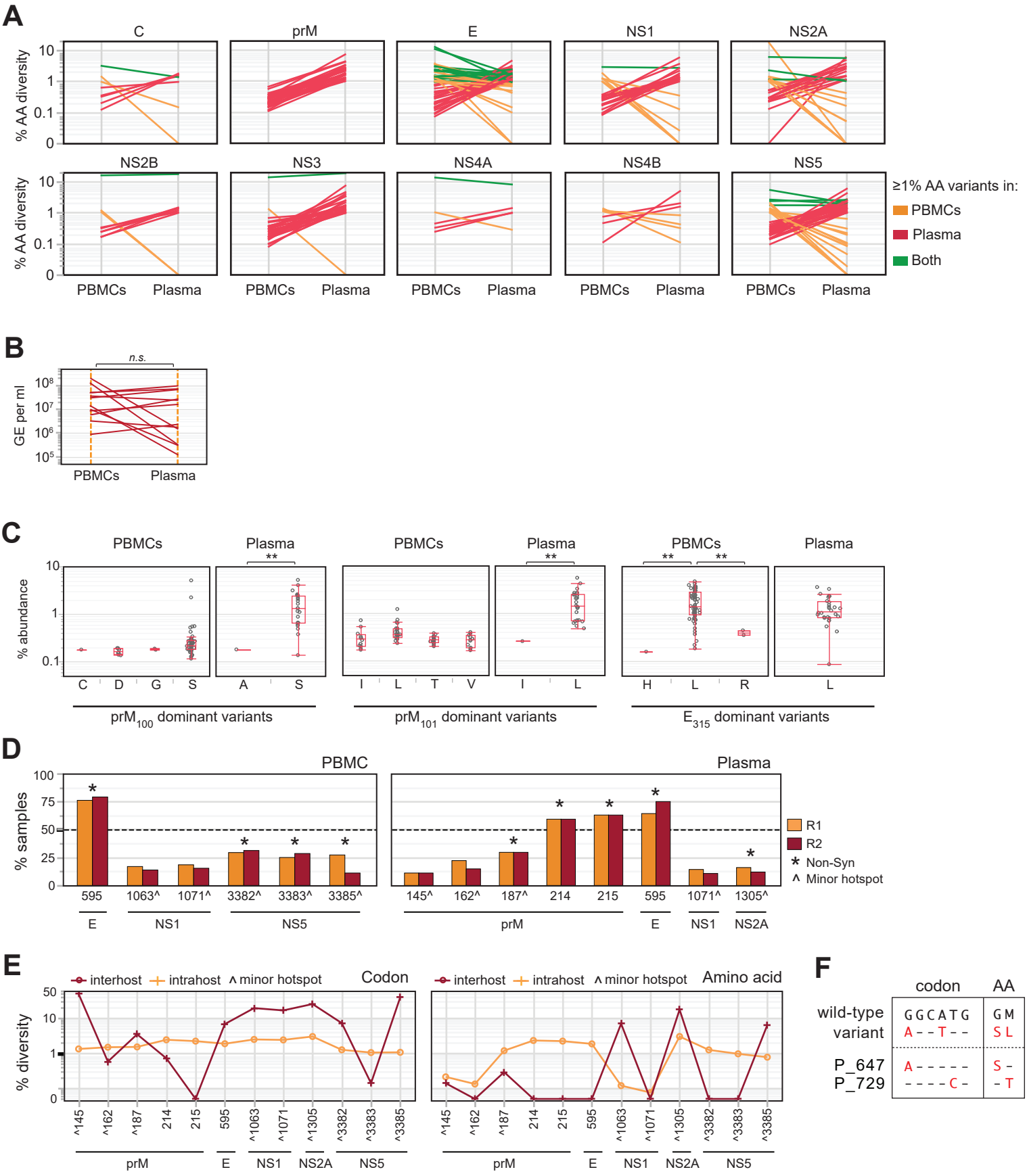
A
C
prM
E
NS1
NS2A
NS2B
NS3
NS4A
NS4B
NS5
% AA diversity
PBMCs
Plasma
≥1% AA variants in:
PBMCs
Plasma
Both
B
n.s.
GE per ml
C
% abundance
**
C D G S A S
I L T V I L
H L R L
prM100 dominant variants
prM101 dominant variants
E315 dominant variants
D
PBMC
Plasma
% samples
595 1063^ 1071^ 3382^ 3383^ 3385^
145^ 162^ 187^ 214 215 595 1071^ 1305^
E NS1 NS5
prM E NS1 NS2A
R1
R2
Non-Syn
Minor hotspot
E
interhost
intrahost
minor hotspot
Codon
Amino acid
% diversity
^145 ^162 ^187 214 215 595 ^1063 ^1071 ^1305 ^3382 ^3383 ^3385
prM E NS1 NS2A NS5
F
codon
AA
wild-type
variant
GGCATG
A--T--
GM
SL
P_647
P_729
A-----
----C-
S-
-T

Figure S3

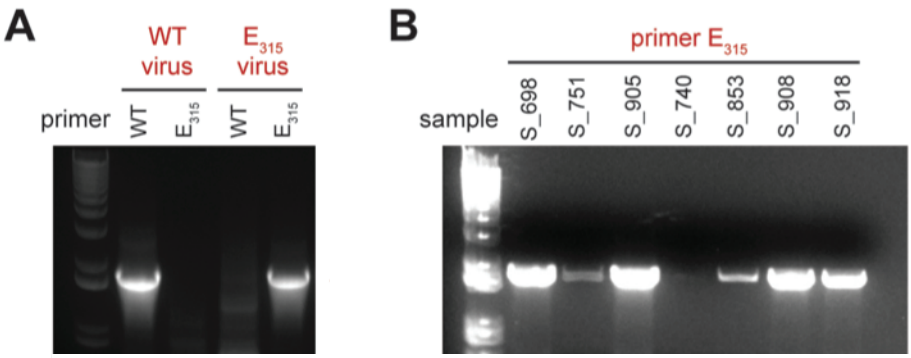
A
WT virus
E315 virus
primer
WT
E315
WT
E315
B
primer E315
sample
S_698
S_751
S_905
S_740
S_853
S_908
S_918

Figure S4

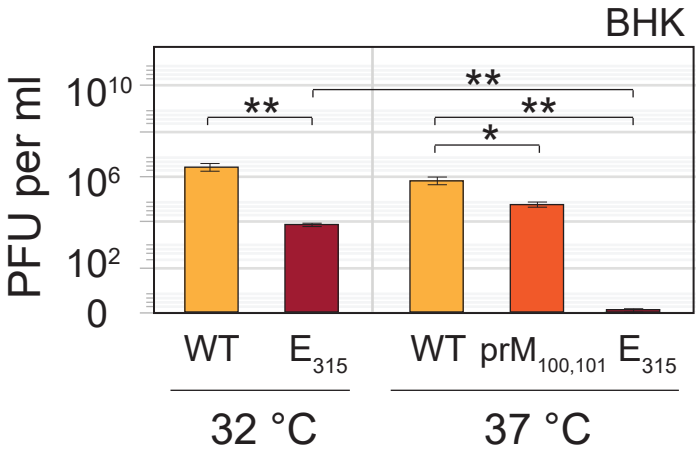

Figure S5

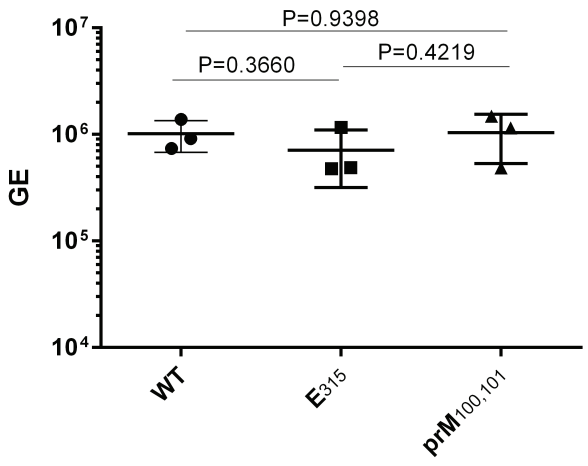

Supplemental Figure Legends

Figure S1. Defining thresholds for intrahost DENV-3 diversity, related to STAR Methods. (A) Sequence-directed capture of intrahost diversity in the DENV-3 coding region using twelve overlapping PCR amplicons. **(B)** For each subset of loci associated with discrete categories of percent variant diversity in replicate A (x-axis), the percent loci in replicate B exhibiting no variants is shown (y-axis). Data is pooled from replicate datasets for four PBMC (*left panels*) and three plasma (*right panels*) samples. Variant diversity is binned by read orientation (read 1 – red and read 2 - yellow), and by type of locus - nucleotide (*top panel*), codon (*middle panel*) or amino acid (*bottom panel*). The threshold for variant detection was chosen based on the minimum percent variant diversity in replicate A at which variants were also detected in replicate B (i.e., the % loci with no variants in replicate B equaled zero), for both reads 1 and 2. **(C)** Frequency distributions of loci in replicate B (y-axis) categorized by percent variant diversity (shades of red), for different cutoffs of percent variant diversity in replicate A (x-axis). Variant diversity is shown for replicate data from four PBMC (*left panels*) and three plasma (*right panels*) samples, and is binned by read orientation (read 1 or read 2) and type of locus - nucleotide (*top panel*), codon (*middle panel*) or amino acid (*bottom panel*).

Figure S2. Diversity profiles in PBMC and plasma samples at the gene and codon levels, related to Figure 1-3. (A) Gene-specific comparisons of percent amino acid variants in paired PBMC and plasma samples, colored by whether individual loci display ≥1% AA diversity in PBMC samples only (yellow), in plasma samples only (red), or in both PBMC and plasma samples (green). **(B)** Comparisons of genome equivalents per milliliter (GE per ml) of extracted RNA in paired PBMC and plasma samples. '*n.s.*' non-significant (Wilcoxon signed-rank test for paired samples). **(C)** Percent abundance of dominant non-synonymous variants observed in PBMC and plasma samples at the prM_{100}, prM_{101} and E_{315} hotspot loci, median ± SD, boxes represent 25^{th} and 75^{th} percentiles, and whiskers are 10^{th} and 90^{th} percentiles. ***P*<0.0001 (Wilcoxon test for unpaired samples). **(D)** All hotspot loci (i.e., loci with ≥1% variant abundance in ≥10% of samples) in PBMC (*left panel*) and plasma (*right panel*) samples in

both read orientations (read 1 in yellow, and read 2 in red). Locus numbering reflects codon position in the DENV-3 polyprotein such that the dominant hotspots prM_{100}, prM_{101} and E_{315} are assigned codon numbers 214, 215 and 595, respectively. Hotspots associated with non-synonymous variants (i.e., mutations that change amino acid sequence) are highlighted with asterisks (*). The dotted line indicates the threshold for identifying the prominent hotspots (i.e., presence of hotspot in ≥50% of samples) in prM and E. Minor hotspot variants are indicated with '^'. **(E)** Average percent intrahost (red) and percent interhost (yellow) diversity in codon (*left panel*) or amino acid (*right panel*) coordinates for each hotspot locus. Interhost diversity was calculated across all global DENV-3 isolates for which full-genome sequences were available (*n* = 690). Minor hotspot variants are indicated with '^'. **(F)** Intermediate and/or alternate nucleotide and amino acid variants for the $prM_{100,101}$ hotspot loci.

Figure S3. Detection of E_{315} variant virus using Reverse Transcription and PCR (RT-PCR), related to Figure 2. (A) RT-PCR using reverse primers specific for wild-type virus (WT) or E_{315} variant virus (E_{315}) yielded an amplified product that was 1865 nucleotide (nt) in length, from WT virus RNA template only, or E_{315} variant virus RNA template only, respectively. Both WT and E_{315} viruses were generated from infectious clones. **(B)** RT-PCR performed using the reverse primer specific for E_{315} variant virus (primer E_{315}) on RNA templates extracted from a randomly-chosen subset of 7 serum samples, yielded amplified product of 1865 nt from all samples.

Figure S4. Phenotype of wild-type, $prM_{100,101}$ and E_{315} variant viruses, related to Figure 4. Plaque forming units per milliliter (PFU/ml) of C6/36-passaged WT and E_{315} viruses at 32°C and 37°C, and $prM_{100,101}$ virus at 37°C, in BHK-21 cells. No plaques were detected for the E_{315} variant virus at 37°C. Data represent the mean ± SD. *P<0.01 and **P<0.0001 (t-test).

Figure S5. Entry capabilities of wild-type, $prM_{100,101}$ and E_{315} variant viruses, related to Figure 4. Entry assays were performed by incubating the WT, E_{315} variant, and $prM_{100,101}$ variant viruses with U937 cells at 37°C for two hours, followed by extensive washing. Viruses were quantified by qRT-PCR

and the Genome Equivalent (GE) values were plotted on the Y-axis, mean ± SD. *P*-values for the various comparisons were computed using a *t*-test.

Supplemental Tables

Table S1. Percent coverage across the DENV-3 genome for each patient sample, related to Table 1.

Sample type	Patient ID^#	Age in Years	Immune status	Disease severity	Sex	Sample collection date	% coverage (read 1)*	Average codon coverage (read 1)*	% coverage (read 2)*	Average codon coverage (read 2)*
PBMC	645	1	Primary	DF	M	09/06/2009	98.32	24357	98.10	20514
PBMC	698	7	Primary	DF	M	09/17/2009	99.71	23355	99.69	21379
PBMC	708	8	Primary	DF	F	09/25/2009	94.88	12353	94.30	10541
PBMC	716	3	Primary	DF	F	10/01/2009	98.73	7972.5	98.28	7655
PBMC	718	9	Primary	DF	F	10/04/2009	99.22	27086.5	99.22	24837.5
PBMC	729	14	Primary	DF	F	10/11/2009	99.10	19225	99.10	17433
PBMC	748	10	Primary	DF	F	09/25/2009	56.61	6716	55.50	6308
PBMC	751	10	Primary	DF	M	09/30/2009	98.33	26492	98.26	23950
PBMC	760	2	Primary	DF	M	10/05/2009	99.37	20094	99.36	18601.5
PBMC	765	5	Primary	DF	M	10/13/2009	99.72	29693.5	99.72	26486.5
PBMC	789	1	Primary	DF	M	10/13/2009	91.38	27174	90.88	25142.5
PBMC	828	5	Primary	DF	F	10/21/2009	90.18	8497	88.94	7891.5
PBMC	831	4	Primary	DF	F	10/20/2009	70.62	9696	66.54	7539
PBMC	832	3	Primary	DF	M	10/20/2009	98.13	29959	98.00	22980
PBMC	839	3	Primary	DF	F	10/23/2009	99.77	27094	99.66	22461.5
PBMC	844	2	Primary	DF	M	10/25/2009	99.49	23128	99.30	18748
PBMC	849	12	Primary	DF	M	10/26/2009	99.52	23127	99.47	19292
PBMC	905	6	Primary	DF	M	11/18/2009	99.70	20021	99.49	15207
PBMC	921	3	Primary	DF	F	11/28/2009	88.41	9714.5	87.74	8234
PBMC	922	7	Primary	DF	F	12/07/2009	88.73	8719	87.30	7408
PBMC	924	2	Primary	DF	M	12/07/2009	99.26	21616	98.99	17800.5
PBMC	927	6	Primary	DF	M	11/19/2009	99.71	18250	99.62	14752
PBMC	934	10	Primary	DF	M	11/28/2009	99.11	16879	98.93	14792.5
PBMC	938	9	Primary	DF	M	11/29/2009	99.72	32155.5	99.69	27281
PBMC	939	10	Primary	DF	F	12/07/2009	99.49	41328.5	99.43	35533.5
PBMC	944	8	Primary	DF	M	12/11/2009	99.88	22253	99.86	19311
PBMC	947	4	Primary	DF	F	12/12/2009	99.88	34318.5	99.88	30020
PBMC	950	4	Primary	DF	M	12/12/2009	98.68	32089	98.65	27836
PBMC	950R	4	Primary	DF	M	12/12/2009	98.57	28363	98.53	25061
PBMC	955	3	Primary	DF	M	12/19/2009	99.24	31680	99.24	27881.5
PBMC	955R	3	Primary	DF	M	12/19/2009	98.44	23452	98.40	21361
PBMC	956	1	Primary	DF	F	12/20/2009	99.89	34099	99.89	31041
PBMC	957	3	Primary	DF	F	12/18/2009	99.88	46762	99.88	42269.5
PBMC	957R	3	Primary	DF	F	12/18/2009	98.82	79693.5	98.81	69010.5
PBMC	1005	9	Primary	DF	M	01/17/2010	99.87	57352	99.86	50548
PBMC	1005R	9	Primary	DF	M	01/17/2010	98.67	30928	98.65	28224
PBMC	647	6	Primary	DHF	M	09/18/2009	77.77	5968	76.93	5009
PBMC	710	6	Primary	DHF	M	09/25/2009	99.52	20294	99.52	17935

PBMC	801	2	Primary	DHF	F	10/26/2009	98.58	32990.5	98.56	30312.5
PBMC	699	7	Primary	DSS	M	09/18/2009	97.54	15235	97.50	13659.5
PBMC	949	9	Primary	DSS	M	12/12/2009	99.64	22635	99.62	20165
PBMC	631	6	Secondary	DF	M	09/07/2009	66.10	6100	62.62	5751
PBMC	632	6	Secondary	DF	M	09/07/2009	98.05	18262	97.95	16261
PBMC	646	5	Secondary	DF	F	09/19/2009	95.93	5822	94.40	4982.5
PBMC	652	8	Secondary	DF	F	09/29/2009	96.80	8873	96.59	7706.5
PBMC	655	11	Secondary	DF	M	10/04/2009	65.73	6552	61.93	6103
PBMC	656	9	Secondary	DF	F	10/05/2009	99.03	18862	99.01	16160
PBMC	694	10	Secondary	DF	M	09/23/2009	98.53	23765	98.51	20980
PBMC	697	6	Secondary	DF	M	09/20/2009	99.69	15933	99.67	14163.5
PBMC	714	8	Secondary	DF	F	09/29/2009	98.24	26650	98.17	23905
PBMC	715	10	Secondary	DF	F	09/28/2009	96.94	20799	96.88	19146
PBMC	722	12	Secondary	DF	F	10/09/2009	75.16	3192	71.88	3037
PBMC	726	6	Secondary	DF	M	10/10/2009	98.94	18862	98.96	16855
PBMC	737	12	Secondary	DF	M	10/12/2009	98.98	25059	98.83	21842
PBMC	740	4	Secondary	DF	F	10/12/2009	99.44	14024	99.09	12111.5
PBMC	792	6	Secondary	DF	F	10/19/2009	57.97	6185	57.35	5689
PBMC	793	7	Secondary	DF	M	10/19/2009	99.22	20080	99.14	18858.5
PBMC	825	10	Secondary	DF	F	10/19/2009	99.63	41146	99.35	36957
PBMC	830	10	Secondary	DF	F	10/20/2009	99.24	16291.5	96.02	12751
PBMC	843	10	Secondary	DF	M	10/24/2009	95.98	44036	95.95	38892
PBMC	853	12	Secondary	DF	F	10/26/2009	99.72	22125	99.59	17492
PBMC	918	8	Secondary	DF	F	11/16/2009	99.12	14107	98.73	11335
PBMC	946	7	Secondary	DF	F	12/12/2009	99.71	22971.5	99.70	19424
PBMC	989	5	Secondary	DF	M	01/27/2010	99.59	11506.5	99.50	10864
PBMC	728	12	Secondary	DHF	M	10/09/2009	88.70	14226	88.67	12810
PBMC	731	5	Secondary	DHF	F	10/10/2009	86.95	36923	86.83	33841
PBMC	833	10	Secondary	DHF	M	10/22/2009	99.57	28447.5	99.43	23109.5
PBMC	848	8	Secondary	DHF	M	10/26/2009	99.58	22216.5	99.36	16733.5
PBMC	937	12	Secondary	DHF	M	11/29/2009	99.72	25700	99.71	21772
PBMC	959	4	Secondary	DHF	F	01/04/2010	98.59	26513.5	98.54	23619
PBMC	717	12	Secondary	DSS	F	10/04/2009	99.26	37144	99.26	30921
PBMC	847	10	Secondary	DSS	F	10/24/2009	97.57	28295	97.56	23012
Plasma	698	7	Primary	DF	M	09/17/2009	99.32	30860	99.04	24554
Plasma	718	9	Primary	DF	F	10/04/2009	99.65	22817.5	99.63	20161
Plasma	751	10	Primary	DF	M	09/30/2009	97.55	8484.5	97.45	7150
Plasma	763	7	Primary	DF	F	10/07/2009	88.76	15506	88.76	13640
Plasma	832	3	Primary	DF	M	10/20/2009	85.72	9447	77.49	19887
Plasma	844	2	Primary	DF	M	10/25/2009	99.34	28214	99.32	22459.5
Plasma	849	12	Primary	DF	M	10/26/2009	76.70	7388.5	76.56	5946.5
Plasma	863	6	Primary	DF	F	10/31/2009	50.75	41668	50.72	30857
Plasma	887	2	Primary	DF	M	11/09/2009	51.42	56349	51.35	48253
Plasma	897	4	Primary	DF	F	11/15/2009	97.34	11099	96.92	9293
Plasma	905	6	Primary	DF	M	11/18/2009	99.67	25622	99.67	23884
Plasma	909	5	Primary	DF	M	11/02/2009	97.46	40600.5	97.43	36203
Plasma	927	6	Primary	DF	M	11/19/2009	99.77	15265	99.71	13156

Plasma	938	9	Primary	DF	M	11/29/2009	99.92	26900.5	99.90	22439
Plasma	939	10	Primary	DF	F	12/07/2009	99.74	21931	99.72	20123
Plasma	944	8	Primary	DF	M	12/11/2009	99.82	36336	99.82	33207
Plasma	646	5	Secondary	DF	F	09/19/2009	99.80	9317	99.75	7654.5
Plasma	656	9	Secondary	DF	F	10/05/2009	99.79	23477	99.72	19973
Plasma	697	6	Secondary	DF	M	09/20/2009	89.64	29521	89.35	25767
Plasma	722	12	Secondary	DF	F	10/09/2009	99.47	21656	99.44	18554.5
Plasma	722R	12	Secondary	DF	F	10/09/2009	92.62	13972	91.91	12277.5
Plasma	737	12	Secondary	DF	M	10/12/2009	88.33	14093	88.27	11744
Plasma	740	4	Secondary	DF	F	10/12/2009	95.24	10473	92.92	9816
Plasma	742	9	Secondary	DF	F	10/13/2009	98.52	19365.5	98.43	16830
Plasma	830	10	Secondary	DF	F	10/20/2009	51.28	41408	51.33	36802
Plasma	853	12	Secondary	DF	F	10/26/2009	99.42	83233	99.35	73919
Plasma	868	13	Secondary	DF	M	11/02/2009	84.87	58334	83.43	51339
Plasma	908	9	Secondary	DF	F	11/04/2009	93.88	18502	91.27	16125
Plasma	918	8	Secondary	DF	F	11/16/2009	99.95	43136	99.96	40261
Plasma	936	14	Secondary	DF	M	11/30/2009	98.50	31324.5	98.50	27792
Plasma	936R	14	Secondary	DF	M	11/30/2009	99.71	28621.5	99.71	26402
Plasma	937	12	Secondary	DHF	M	11/29/2009	99.82	22978.5	99.81	20074
Plasma	847	10	Secondary	DSS	F	10/24/2009	99.74	27811	99.71	24865.5
Plasma	847R	10	Secondary	DSS	F	10/24/2009	99.90	57468	99.90	51485

^The suffix ‘R’ denotes replicate sample used in defining thresholds for percent intrahost diversity.

[#]All samples used for this study were from individuals who presented with DENV-3 infection during the 2009-2010 epidemic season in Nicaragua. Over 100 other clinical and laboratory parameters are available for these samples, but not shown due to space constraints.

*Only nucleotide loci with coverage of ≥1000 reads and locus-specific Sanger quality scores of ≥30 were considered for calculating genome coverage. Samples with ≥50% genome coverage are reported.

Table S2. Interhost diversity at hotspots for intrahost diversity, related to Figure 2.

Codon position	Primary[#] codons (intrahost)	Variant* codons (intrahost)	Primary[#] codons (interhost^)	Variant* codons (interhost^)	Primary[#] AA (intrahost)	Variant* AA (intrahost)	Primary[#] AA (interhost^)	Variant* AA (interhost^)
145	ATT, ATC	ATC, ATT	ATC	ATT, (ACT)	I	V, (T)	I	T
162	ACG, ACA	ACA, ACG	ACG	ACA	T	A	T	-
187	ACA	GCT, GCA, (ACT)	ACA	ACG, (GCA, GCG)	T	A	T	A
214	GGC	AGC	GGC	GGT	G	S	G	-
215	ATG	TTG	ATG	-	M	L	M	-
595	CAT	CTT	CAT	CAC	H	L	H	-
1063	AAT, AAC	AAC, AAT	AAC	AAT, AGC, (GAC, GAT)	N	S, (K, D, H, I, T)	N	S, D
1071	TTA, TTG	TTG, TTA	TTG	CTG, TTA	L	F, S, (*, V, I)	L	-
1305	GTG, ATG	GCG, GTG, ATG, GTA	GTG	CTG, ATG, (TTG, GTA)	V, M	A, M, V	V	L, M
3382	GAG	GGG	GAG	GAA	E	G	E	-
3383	GAG	GGG	GAG	GAA	E	G	E	-
3385	TCG	TTG, TCA	TCG	TCA, TTG, (ACA, TTA, CCA)	S	L	S	L, T, (P)

^For calculating interhost diversity, all available full-length DENV-3 genomes from global isolates (*n* = 690) were used

[#]Codons and amino acids with the highest prevalence are listed as ‘primary’

*Minor codons and amino acids are listed as ‘variant’ (in decreasing order of prevalence)

Table S3. Frequencies of various haplotypes linked to variants at the $prM_{100,101}$ and E_{315} hotspot loci, related to Figure 3.

Variant	Haplotypes linked to variant	Frequency (predicted)^	Frequency (observed)[#]	Number of samples with variant haplotype identical to wild-type consensus haplotype (percent of all samples with variant haplotype)
$prM_{100,101}$	C-G-C	0.702	0.688	3 (100%)
$prM_{100,101}$	T-G-C	0.170	0.195	2 (100%)
$prM_{100,101}$	C-A-C	0.093	0.104	2 (100%)
$prM_{100,101}$	C-A-T	0.001	0.013	1 (100%)
E_{315}	G-G-A	0.533	0.636	24 (100%)
E_{315}	A-G-A	0.304	0.195	7 (100%)
E_{315}	A-A-A	0.040	0.117	4 (100%)
E_{315}	A-G-G	0.017	0.052	4 (100%)

^Product of the frequencies of alleles at each of the three loci, calculated from Nicaraguan consensus DENV-3 genomes used in this study.

[#]Frequencies of haplotypes observed in Nicaraguan consensus DENV-3 genomes used in this study.

Table S4. Sequences of primers used for amplifying the DENV-3 genome, related to STAR Methods.

Sequence	Description	Tm	Amplicon#	Comments
GACTCGGAAGCTTGCTTAAC	DENV3_32_F	62.00	DENV3-Amplicon1	
TGATCCAAAGTCCCAAGCTG	DENV3_2196_R	61.18		
TCAATATGCTGAAACGCGTG	DENV3_128_F	60.81	DENV3-Amplicon2	
TGATCCAAAGTCCCAAGCTG	DENV3_2196_R	61.18		
AAGCTATGCATTGAGGGGAA	DENV3_1106_F	60.04	DENV3-Amplicon3	
GTATCGCAAGGGAGGRAGTG	DENV3_3378_R	59.69		
CATATGGCTGAAACTCCGAG	DENV3_2907_F	58.33	DENV3-Amplicon4	
CCAAGCACAAGACACCCATT	DENV3_3511_R	60.95		
GGARGTGGAAAGGTGGACAA	DENV3_3466_F	59.94	DENV3-Amplicon5	R=A or G
ATRCTGGCTGGGTCTGTGAA	DENV3_5393_R	58.16		
TTGACTGTTGCCTGGAGAAC	DENV3_3946_F	58.85	DENV3-Amplicon6	
CGTCTATGGCGGCYGACTT	DENV3_6073_R	59.46		
AAACGAACGCAGAACCAGAT	DENV3_5009_F	59.74	DENV3-Amplicon7	
GCGTACAATGTCCAGGCTGA	DENV3_6941_R	60.47		
CTCGTGTTGGAATGGGAGAG	DENV3_5417_F	60.17	DENV3-Amplicon8	
ACAYAAGGCCCATGATGTTC	DENV3_7389_R	60.79		
GTCAATCRCCCTTGATCTTG	DENV3_6366_F	60.60	DENV3-Amplicon9	R=G or A
ATGTTACCTGTRCCATTGGA	DENV3_8240_R	58.85		
CGGTRGATGGGATAATGACA	DENV3_7253_F	61.53	DENV3-Amplicon10	R=G or A
CTCCGGGTATCTTGGAAATG	DENV3_9139_R	59.38		
ATCCAATGGYACAGGTAACA	DENV3_8220_F	58.85	DENV3-Amplicon11	Y=T or C
GATTGTCCTCGATCCACACC	DENV3_10024_R	60.33		
ATGGATCTTATGAAGTCAAAGC	DENV3_8478_F	58.86	DENV3-Amplicon12	
ACTGTGGCTTAATRTGGCCT	DENV3_10302_R	59.62		